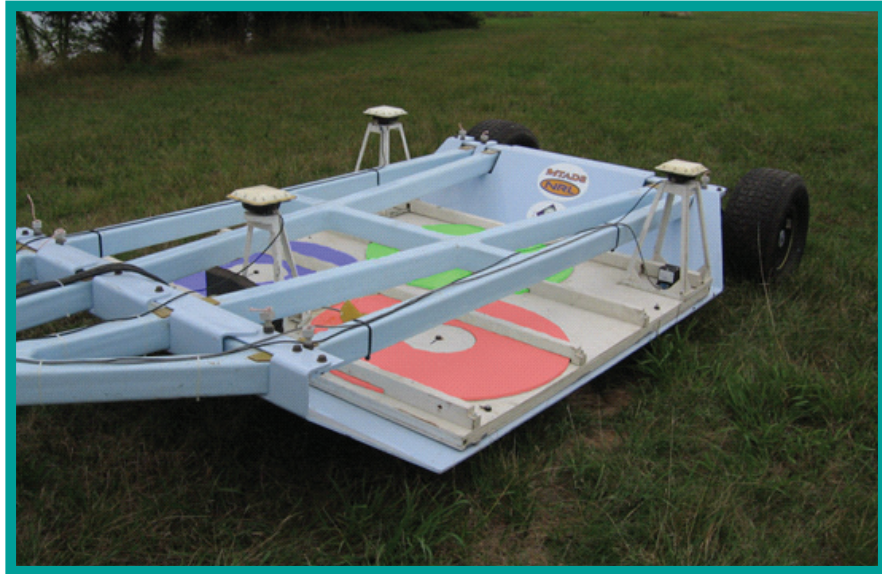


# ESTCP Cost and Performance Report

(MM-0033)



## Enhanced UXO Discrimination Using Frequency Domain Electromagnetic Induction

May 2010



ENVIRONMENTAL SECURITY  
TECHNOLOGY CERTIFICATION PROGRAM

U.S. Department of Defense

# Report Documentation Page

Form Approved  
OMB No. 0704-0188

Public reporting burden for the collection of information is estimated to average 1 hour per response, including the time for reviewing instructions, searching existing data sources, gathering and maintaining the data needed, and completing and reviewing the collection of information. Send comments regarding this burden estimate or any other aspect of this collection of information, including suggestions for reducing this burden, to Washington Headquarters Services, Directorate for Information Operations and Reports, 1215 Jefferson Davis Highway, Suite 1204, Arlington VA 22202-4302. Respondents should be aware that notwithstanding any other provision of law, no person shall be subject to a penalty for failing to comply with a collection of information if it does not display a currently valid OMB control number.

1. REPORT DATE <b>MAY 2010</b>		2. REPORT TYPE		3. DATES COVERED <b>00-00-2010 to 00-00-2010</b>	
4. TITLE AND SUBTITLE <b>Enhanced UXO Discrimination Using Frequency Domain Electromagnetic Induction</b>				5a. CONTRACT NUMBER	
				5b. GRANT NUMBER	
				5c. PROGRAM ELEMENT NUMBER	
6. AUTHOR(S)				5d. PROJECT NUMBER	
				5e. TASK NUMBER	
				5f. WORK UNIT NUMBER	
7. PERFORMING ORGANIZATION NAME(S) AND ADDRESS(ES) <b>Strategic Environmental Research and Development Program (SERDP), Environmental Security Technology Certification Program (ESTCP), 4800 Mark Center Drive, Suite 17D08, Alexandria, VA, 22350-3605</b>				8. PERFORMING ORGANIZATION REPORT NUMBER	
9. SPONSORING/MONITORING AGENCY NAME(S) AND ADDRESS(ES)				10. SPONSOR/MONITOR'S ACRONYM(S)	
				11. SPONSOR/MONITOR'S REPORT NUMBER(S)	
12. DISTRIBUTION/AVAILABILITY STATEMENT <b>Approved for public release; distribution unlimited</b>					
13. SUPPLEMENTARY NOTES					
14. ABSTRACT					
15. SUBJECT TERMS					
16. SECURITY CLASSIFICATION OF:			17. LIMITATION OF ABSTRACT <b>Same as Report (SAR)</b>	18. NUMBER OF PAGES <b>62</b>	19a. NAME OF RESPONSIBLE PERSON
a. REPORT <b>unclassified</b>	b. ABSTRACT <b>unclassified</b>	c. THIS PAGE <b>unclassified</b>			

**COST & PERFORMANCE REPORT**  
**Project: MM-0033**

**TABLE OF CONTENTS**

	<b>Page</b>
1.0 EXECUTIVE SUMMARY .....	1
1.1 BACKGROUND.....	1
1.2 OBJECTIVES OF THE DEMONSTRATION .....	1
1.3 DEMONSTRATION RESULTS.....	1
1.4 IMPLEMENTATION ISSUES.....	2
2.0 INTRODUCTION.....	3
2.1 BACKGROUND.....	3
2.2 OBJECTIVES OF THE DEMONSTRATION .....	4
2.3 REGULATORY DRIVERS.....	4
3.0 TECHNOLOGY .....	5
3.1 TECHNOLOGY DESCRIPTION .....	5
3.2 ADVANTAGES AND LIMITATIONS OF THE TECHNOLOGY .....	6
4.0 PERFORMANCE OBJECTIVES.....	7
4.1 OBJECTIVE: PROBABILITY OF DETECTION .....	7
4.1.1 Metric.....	7
4.1.2 Data Requirements .....	8
4.1.3 Success Criteria .....	8
4.1.4 Results .....	8
4.2 OBJECTIVE: FALSE ALARM RATE .....	9
4.2.1 Metric.....	9
4.2.2 Data Requirements .....	10
4.2.3 Success Criteria .....	10
4.2.4 Results .....	10
4.3 OBJECTIVE: ARRAY SNR.....	10
4.3.1 Metric.....	11
4.3.2 Data Requirements .....	11
4.3.3 Success Criteria .....	11
4.3.4 Results .....	11
4.4 OBJECTIVE: RELIABILITY .....	17
4.4.1 Metric.....	17
4.4.2 Data Requirements .....	17
4.4.3 Success Criteria .....	17
4.4.4 Results .....	17
4.5 OBJECTIVE: EASE OF USE .....	17
4.5.1 Metric.....	17
4.5.2 Data Requirements .....	17

## TABLE OF CONTENTS (continued)

	<b>Page</b>
4.5.3 Success Criteria .....	17
4.5.4 Results .....	18
4.6 OBJECTIVE: MAINTENANCE .....	18
4.6.1 Metric.....	18
4.6.2 Data Requirements .....	18
4.6.3 Success Criteria .....	18
4.6.4 Results .....	18
5.0 SITE DESCRIPTION.....	19
5.1 SITE LOCATION AND HISTORY.....	19
5.1.1 Climate and Weather .....	19
5.1.2 Topography .....	19
5.1.3 Site Maps and Photographs .....	20
5.2 MUNITIONS CONTAMINATION .....	21
6.0 TEST DESIGN .....	23
6.1 CONCEPTUAL EXPERIMENTAL DESIGN .....	23
6.2 SITE PREPARATION.....	23
6.3 SYSTEMS SPECIFICATION .....	23
6.3.1 MTADS Tow Vehicle.....	23
6.3.2 GEM-3 (GEMTADS) Array .....	24
6.4 DATA COLLECTION .....	27
6.4.1 Scale of Demonstration .....	27
6.4.2 Sample Density.....	27
6.4.3 Quality Checks .....	27
6.4.4 Data Summary .....	28
6.5 VALIDATION .....	28
7.0 DATA ANALYSIS AND PRODUCTS .....	29
7.1 PREPROCESSING.....	29
7.2 TARGET SELECTION FOR DETECTION.....	30
7.3 PARAMETER ESTIMATES .....	30
7.4 CLASSIFIER AND TRAINING .....	31
7.5 DATA PRODUCTS.....	31
8.0 PERFORMANCE ASSESSMENT .....	33
8.1 ABERDEEN PROVING GROUND BLIND GRID .....	33
8.1.1 Response Stage.....	33
8.1.2 Discrimination Stage .....	36
8.2 ABERDEEN PROVING GROUND OPEN FIELD .....	38
8.2.1 Response Stage.....	39
8.2.2 Discrimination Stage .....	40
8.3 YUMA PROVING GROUND OPEN FIELD .....	41

## TABLE OF CONTENTS (continued)

	<b>Page</b>
8.3.1 Response Stage .....	41
8.3.2 Discrimination Stage .....	42
9.0 COST ASSESSMENT .....	43
9.1 COST MODEL .....	43
9.2 COST DRIVERS .....	43
9.3 COST BENEFIT.....	43
10.0 IMPLEMENTATION ISSUES.....	45
11.0 REFERENCES.....	47
APPENDIX A      POINTS OF CONTACT.....	A-1

*This page left blank intentionally.*

## LIST OF FIGURES

		Page
Figure 1.	MTADS GEM-3 array mounted on the EM sensor trailer. ....	5
Figure 2.	GEMTADS background noise levels as measured at the three demonstration sites.....	11
Figure 3.	In-phase and quadrature response as a function of frequency for eight of the APG UXO set and the GEMTADS array. ....	13
Figure 4.	In-phase and quadrature response as a function of frequency for five of the APG UXO set and the GEMTADS array. ....	14
Figure 5.	GEMTADS across-axis quadrature response, averaged over mid-frequencies for eight of the APG ordnance items as a function of depth. ....	15
Figure 6.	GEMTADS across-axis quadrature response, averaged over mid-frequencies for five of the APG ordnance items as a function of depth. ....	16
Figure 7.	Aerial photograph of the Aberdeen Test Site with the various scenarios outlined. ....	20
Figure 8.	Aerial photograph of the Yuma Test Site with the various scenarios outlined. ....	21
Figure 9.	Schedule of field testing activities. ....	23
Figure 10.	MTADS GEM-3 array in operation pulled by the MTADS tow vehicle. ....	24
Figure 11.	MTADS EM trailer with approximate locations of GPS and IMU equipment indicated. ....	25
Figure 12.	Schematic of interleaved survey pattern for GEMTADS surveys.....	26
Figure 13.	GEM-3 array control electronics and GPS receivers.....	26
Figure 14.	Working screen of the WinGEM2kArr program. ....	27
Figure 15.	A schematic diagram showing the integration of the GEM and navigation data for eventual analysis.....	29
Figure 16.	$Q_{avg}$ anomaly image map of the APG Blind Grid.....	34
Figure 17.	$Q_{avg}$ detection performance as a function of depth at the APG Blind Grid. ....	35
Figure 18.	Response stage results showing cumulative ordnance count versus cumulative clutter.....	35
Figure 19.	Response stage performance showing cumulative occupied cell count plotted versus adjusted cumulative blank cell count.....	36
Figure 20.	ROC curve for the $\chi^2$ weighting applied to the APG Blind Grid as shown in the left-hand side of Figures 25 and 26 of Reference 8. ....	37
Figure 21.	ROC curve for the case of $\chi^2$ weighting with an estimate of “bouncing noise” included applied to the APB Blind Grid.....	38
Figure 22.	ROC curve for the $\chi^2$ ratio method applied to the APG Blind Grid.....	38
Figure 23.	Detection performance at the APG Open Field scenario.....	39
Figure 24.	Response stage results for the APG Open Field scenario broken out by target type.....	40
Figure 25.	Discrimination performance at the APG Open Field scenario. ....	40
Figure 26.	Detection performance at the YPG Open Field scenario.....	41
Figure 27.	Response stage results for the YPG Open Field scenario broken out by target type.....	42
Figure 28.	Discrimination performance at the YPG Open Field scenario. ....	42

## LIST OF TABLES

	<b>Page</b>
Table 1.	Performance objectives for the demonstration. .... 7
Table 2.	GEMTADS Blind Grid Test Area response stage $P_d$ results. .... 8
Table 3.	GEMTADS Blind Grid Test Area response stage $P_{fp}$ and $P_{ba}$ results..... 9
Table 4.	GEMTADS Open Field Test Area response stage $P_d$ results..... 9
Table 5.	GEMTADS Open Field Test Area response stage $P_{fp}$ and $P_{ba}$ results..... 9
Table 6.	GEMTADS Blind Grid Test Area efficiency and rejection rates. .... 10
Table 7.	GEMTADS Open Field Test Area efficiency and rejection rates. .... 10
Table 8.	Survey coverage of GEMTADS array at the two test sites. .... 27
Table 9.	Summary of detection performance at the APG Blind Grid..... 33
Table 10.	Summary of Costs for a 50-acre GEM array survey..... 43



## ACRONYMS AND ABBREVIATIONS

---

Al	aluminum
APG	Aberdeen Proving Ground
AMTADS	Airborne Multisensor Towed Array Detection System
ATC	Aberdeen Test Center
DAQ	Data Acquisition (System)
DSP	digital signal processor
EM	electromagnetic
EMI	electromagnetic induction
ESTCP	Environmental Security Technology Certification Program
GEMTADS	MTADS GEM-3 EMI array
GPS	Global Positioning System
Hz	Hertz
IDA	Institute for Defense Analyses
IMU	inertial measurement unit
kHz	kilohertz
MTADS	Multisensor Towed Array Detection System
NMEA	National Marine Electronics Association
NRL	Naval Research Laboratory
$P_{ba}$	probability of background alarm
$P_d$	probability of detection
$P_{fa}$	probability of false alarm
PI	principal investigator
ppm	parts per million
(PTNL,)AVR	Time, Yaw, Tilt, Range for Moving Baseline RTK NMEA-0183 message
(PTNL,)GGK	Time, Position, Position Type, DOP NMEA-0183 message
QC	quality control
$R_{fp}$	false positive rejection rate
rms	root mean square
ROC	receiver operating curve
RTK	real time kinematic
s/n	signal to noise

## ACRONYMS AND ABBREVIATIONS (continued)

---

SAIC	Science Applications International Corporation
SERDP	Strategic Environmental Research and Development Program
SNR	signal-to-noise ratio
USCOE	U.S. Corps of Engineers
UTC	Universal Coordinated Time
UXO	unexploded ordnance
YPG	Yuma Proving Ground

## ACKNOWLEDGEMENTS

This project was a collaborative effort between the Naval Research Laboratory, AETC Inc. (now Science Applications International Corporation [SAIC]), and Geophex Ltd. I.J. Won, Alex Oren, Frank Funak, and Bill San Filippo were responsible for the development of the EMI sensor technology on which the GEMTADS array was built. Tom Bell, Nagi Khadr, and Bruce Barrow of SAIC were responsible for the modeling/analysis of the GEMTADS data. Dan Steinhurst and Glenn Harbaugh of Nova Research Inc. were responsible for the integration of the GEM-3 sensors and electronics into the MTADS platform and the deployment of the system.

*Technical material contained in this report has been approved for public release.*

*This page left blank intentionally.*

## **1.0 EXECUTIVE SUMMARY**

### **1.1 BACKGROUND**

The Chemistry Division of the Naval Research Laboratory (NRL) has participated in several programs funded by the Strategic Environmental Research and Development Program (SERDP) and Environmental Security Technology Certification Program (ESTCP) whose goal has been to enhance the discrimination ability of the Multisensor Towed Array Detection System (MTADS). The process has been based on making use of both the location information inherent in an item's magnetometry response and the shape and size of information inherent in the response to the time-domain electromagnetic induction (EMI) sensors in either a cooperative or joint inversion. In all of these efforts, classification performance has been limited by the information available from the EMI sensor. Prior to this project, the industry-standard EMI sensor, the Geonics EM61, was used. The EM61 is a time-domain instrument with either a single time gate to sample the amplitude of the decaying signal or four time gates sampling relatively early in time.

To make further progress on unexploded ordnance (UXO) classification, a sensor with more information available was required. The Geophex GEM-3 sensor is a frequency-domain sensor with up to 10 frequencies available for simultaneous measurement of the in-phase and quadrature response of the target. In principle, there is much more information available from this sensor for use in UXO classification decisions. The commercial GEM-3 sensor is a handheld instrument not very amenable to rapid, wide area surveys. This project was funded to overcome this limitation through the integration of an array of GEM-3 sensors with the MTADS platform.

### **1.2 OBJECTIVES OF THE DEMONSTRATION**

The objective of this project was to demonstrate the optimum system that delivers the most UXO classification performance possible while retaining acceptable survey efficiency. Working with a modified GEM-3 sensor, we have designed a three-sensor array and demonstrated it at the Standardized UXO Demonstration sites at Aberdeen Proving Ground (APG) and Yuma Proving Ground (YPG). For the Blind Test Grid and the Open Field Areas, our ranked target picks were submitted to the Aberdeen Test Center (ATC) for scoring. These scoring results are the basis for accessing the success of the demonstrations.

### **1.3 DEMONSTRATION RESULTS**

The GEM-3 sensor was selected for this towed array because of its performance at the JPG-IV demonstration in 1998. With the capability of measuring in-phase and quadrature signals at 10 frequencies over the 30 hertz (Hz) to 20 kilohertz (kHz) range, the GEM-3 should have the necessary information to enhance UXO discrimination from clutter more effectively than the current state of the art. Overall, the results from the GEM-3 array described in this report at the Standardized UXO Demonstration Sites were a disappointment.

The GEM-3 array was capable of detecting ordnance to reasonable burial depths. All ordnance was detected on the APG Blind Grid to burial depths equal to 11 times the UXO item's diameter. It was not effective at distinguishing UXO from clutter. Even after adjusting for items emplaced

too deep to be detected, high discrimination probabilities of detection ( $P_d$ ) were achieved only at high levels of probabilities of false alarm ( $P_{fa}$ ).

The primary cause is an issue of signal-to-noise ratio (SNR). Model-based, dipole inversions require fairly high levels of SNR ( $>10$ ) to return reliable results. For the three test sites visited by the system, the average noise levels varied from less than one part-per-million (ppm) for mid-frequency quadrature responses to almost 10 ppm for the in-phase response at all frequencies. The signal level for most of the emplaced ordnance was in the range of 1 to 10's of ppm. This response level is too weak to invert reliable ordnance signatures across all the frequencies for both the in-phase and quadrature responses. Distinguishing ordnance from clutter relies on accurate inversion of the in-phase/quadrature signature and the comparison of this signature to the library of expected ordnance. At low SNR, this is not possible.

Further complicating this library comparison process is the large number and variety of UXO items emplaced at the test sites. Given the error bars on the inverted parameters, there is necessarily a large overlap between UXO and clutter signatures.

It has also been noted that good inversion results from dynamic survey data require accurate positioning of the sensors, on the order of sub-centimeter positioning. The positioning and orientation of the GEM-3 array was provided by a cm-level Global Positioning System (GPS).

#### **1.4 IMPLEMENTATION ISSUES**

Implementation of the methods used in this demonstration requires additional survey time compared to a minimum-effort detection survey. We have shown that the MTADS can detect all UXO of gauges 40 mm or larger with a total-field magnetometry survey alone. For ordnance target sets that include 60- and 81-mm mortars at depths of 0.75 to 1 m and/or 20- and 30-mm submunitions, an overlapping EMI survey is required to generate sufficient data density and to get a high detection probability. This increases the survey hours on site although it does not impact the mobilization and data analysis costs. In many cases, the extra survey costs are only equivalent to the cost of digging one or two additional targets per acre.

The MTADS GEM-3 array is a vehicular-towed array with the operating limitations of a towed system. Support requirements are not extensive. For normal operation, the vehicle and sensor trailer are stored in a garage or a two-door shipping container overnight. Power at the storage site is required to charge the vehicle batteries overnight. Other batteries (sensors, GPS base station, radios, etc.) can be charged off site or in a hotel room. For extended surveys, an office space is procured for the data preprocessor and for serving as an electronics diagnosis and repair area. The minimum survey crew consists of a vehicle driver, one other field helper (for safety considerations), and a data quality control (QC) and preprocessing analyst. As the data preprocessor has time available, target analysis can begin in the field. The bulk of target analysis is typically carried out later at the analyst's office. The addition of a fourth team member who splits time between the field, data analysis, and general troubleshooting is recommended.

## 2.0 INTRODUCTION

### 2.1 BACKGROUND

UXO detection and remediation is a high priority triservice requirement. As the Defense Science Board wrote in 2003, “Today’s UXO cleanup problem is massive in scale with some 10 million acres of land involved. Estimated cleanup costs are uncertain but are clearly tens of billions of dollars. This cost is driven by the digging of holes in which no UXOs are present. The instruments used to detect UXOs (generally located underground) produce many false alarms—i.e., detections from scrap metal or other foreign or natural objects—for every detection of a real unexploded munition found” [1].

There has been considerable progress in the detection of buried UXO in the last 15 years. The MTADS, supported by ESTCP, has demonstrated that UXO items with gauges larger than 20 mm are typically detected to their likely burial depths with location accuracies on the order of 15 cm [2]. To reliably detect the smaller gauge munitions in this spectrum, the MTADS EM61 MkII or GEM-3 arrays should be used rather than the magnetometer array. Discrimination of UXO from ordnance fragments and other clutter remains a problem, however. We have shown that with careful mission planning and a modest on-site training effort, an MTADS survey/remediation project can achieve false alarm rates substantially lower than those quoted for mag-and-flag surveys. However, there is still much room for improvement in discrimination ability that will result in direct reduction of remediation costs.

The Chemistry Division of the NRL has participated in several programs funded by SERDP and ESTCP whose goal has been to enhance the discrimination ability of MTADS. The process has been based on making use of both the location information inherent in an item’s magnetometry response and the shape and size of information inherent in the response to the time-domain electromagnetic induction sensors that are part of the baseline MTADS in either a cooperative or joint inversion. We have already made significant progress toward our goal. The algorithms and methods developed for ESTCP involving analysis of data from the MTADS EM61 array were applied in preliminary form at the JPG-IV Demonstration allowing us to score as one of the small group of approaches that showed any classification ability [3]. More recently, we have used the methods at JPG-V and on a live range, the Impact Area of the Badlands Bombing Range, SD. In all these demonstrations, our classification ability has been limited by the information available from the sensor. The EM61 is a time-domain instrument with a single gate or four gates early in time to sample the amplitude of the decaying signal. To make further progress on UXO classification, a sensor with more information available is required.

By far the best results at JPG-IV were obtained by Geophex and AETC using magnetometers and the GEM-3 frequency-domain electromagnetic induction sensor [3]. The GEM-3 sensor is a frequency-domain sensor with up to 10 frequencies available for simultaneous measurement of the in-phase and quadrature response of the target. Thus, in principle, there is much more information available from a GEM-3 sensor for use in classification decisions. Unfortunately, the commercial GEM-3 sensor is a handheld instrument with relatively slow data rates and is thus not very amenable to rapid, wide area surveys. ESTCP Project 200033, Enhanced UXO

Discrimination Using Frequency-Domain Electromagnetic Induction, was funded to overcome this limitation by integrating an array of GEM-3 sensors with the MTADS platform.

## **2.2 OBJECTIVES OF THE DEMONSTRATION**

The original objective of the demonstration was simple: Demonstrate the classification performance of the GEM-3 sensor in conjunction with the survey efficiency of the MTADS. As we undertook the first task of the program, specification of the sensor configuration most amenable to platform-based array use, we quickly became aware of a significant noise issue with the original GEM-3 sensor when mounted on a cart. Our observations and subsequent modifications to the original sensor are detailed in an earlier report [4].

The revised objective is only slightly more complicated: Demonstrate the optimum system that delivers the most classification performance while retaining acceptable survey efficiency. Working around a modified GEM-3 sensor, we have designed a three-sensor array, which will be described in detail in Sections 2.1 and 5.3, and demonstrated it at the Standardized UXO Demonstration sites at APG and YPG. At each of the sites, we surveyed the Calibration Lanes, the Blind Test Grid, and as much of the Open Field Area as was possible. For the Blind Test Grid and the Open Field, our ranked target picks were submitted to ATC for scoring. These scoring results are the basis for judging the success of the demonstrations.

## **2.3 REGULATORY DRIVERS**

Stakeholder acceptance of the use of discrimination techniques on real sites will require demonstration that these techniques can be deployed efficiently and with high probability of discrimination. The first step in this process is to demonstrate acceptable performance on a test site such as that at APG. After that hurdle has been passed, successful demonstration at a live site will facilitate regulatory acceptance of the methods.



## 3.0 TECHNOLOGY

### 3.1 TECHNOLOGY DESCRIPTION

Each of the GEM-3 sensors in the array sequentially transmits a composite waveform made up of nine frequencies logarithmically spaced from 90 Hz to just over 20 kHz for one base period (1/30 s). Thus, only three complete cycles of the 90 Hz frequency are transmitted while many thousands of cycles of the highest frequency are transmitted. The transmit current drives both a transmit coil and a counterwound bucking coil. This serves to set up a “magnetic cavity” inside the bucking coil, in which a receive coil is placed. The current induced in this receive coil by the induced fields in buried metal targets is detected, digitized, and frequency resolved during the two subsequent base periods while the other array sensors are transmitting. The detected signal is compared to the transmitted current and reported relative to the transmit current (ppm) as both an in-phase and quadrature component.

Based on the lessons learned with the prototype array [4], we arrived at a design for the demonstration array, which is shown in Figure 1. The coils used in the array are 96 cm in diameter with a larger number of turns. New, higher current transmitter electronics were designed and constructed to drive the coils. The product of these two factors results in a factor of six to eight increase in transmit moment. The new sensor electronics bring other benefits as well. We are now able to implement real-time low-pass filtering of the induced current using a digital signal processor (DSP) chip in the receive circuit. This reduces the absolute level of the noise in addition to the relative decrease obtained from the increased transmit moment. Other deployment measures have been taken to reduce the induced noise in the sensor array. The three sensors are mounted on a rigid base attached to the sensor tray to minimize relative motion. We have optimized the sensor cart for a steady ride. This includes making the wheelbase as long as possible and controlling tire pressure. We also deploy an array of GPS receivers to measure orientation of the sensor platform as well as position and a six-axis inertial measurement unit (IMU).



**Figure 1. MTADS GEM-3 array mounted on the EM sensor trailer.**  
Note the three GEM sensors, the three GPS antennae,  
and the IMU for platform motion measurement.

The sensor timing sequence was chosen to be non-synchronous (each sensor operating independently) and sequential. This was done to avoid the expense of developing new drive electronics (the individual GEM-3 sensors are configured to run independently) and the large, unbucked inter-sensor interference that results from simultaneous operation. Inter-sensor sequencing is controlled by the custom electronics package mentioned above.

Sequential operation of the sensors does not cause the large reduction in array sampling rate that might be imagined on first thought. The baseline GEM-3 sensor operates on a 1/30 base period. That is, each sensor acquires data for a multiple of this base period. It then takes approximately two base periods to perform the internal data reduction calculations before the results of the measurement are available to the recording computer. If each of the three sensors in this sequential array is configured to record for a single base period, they can then be run near their maximum rate. The effective sampling rate for the three sensor array is ~9.5 Hz, which coupled with a survey speed of ~3 mph, results in a down-track sampling interval of ~15 cm. This results in an acceptable data density for our analysis purposes.

### **3.2 ADVANTAGES AND LIMITATIONS OF THE TECHNOLOGY**

No single method currently available is the magic bullet of classification. We have previously demonstrated [2] that some discrimination is possible using the standard MTADS if a small training area is investigated prior to data analysis on the entire site and the distribution of ordnance is limited. This discrimination is based primarily on fitted dipole “size.” More recently we have shown that increased discrimination can be achieved by adding an extra “dimension” to the discrimination—that of “shape.” For items of the same induced magnetic dipole, we can discriminate based on the ratio of responses of the items’ three axes to the EMI sensors in the MTADS suite. As we have shown [5], this adds some discrimination capability to the system.

Unfortunately, the EM methods previously demonstrated are not sufficiently robust to the sensor noise, position uncertainty, and platform motion inherent at a real site. We have proposed that some of this observed drop in performance at real sites can be recaptured using a sensor with more inherent information content. The GEM-3 sensor that is the subject of this demonstration is such a sensor. The depth performance of the GEM-3 sensors is limited compared to the time-domain EM sensors we have demonstrated in previous programs due to the reduced transmit moment associated with the non-synchronous transmit mode.

Even with the most optimistic result, however, these methods will not result in a perfect system. As stated many times, this program is based on the idea of classification by shape. By definition, this implies that clutter items that have similar shapes to ordnance will be classified as ordnance. Items such as pipes and post sections are representative of this problem. If it is important to reduce remediation costs to the extent that these items are not dug, other methods, possibly sensitive to composition or the presence of explosive compounds, will have to be employed in conjunction with those being demonstrated in this program.

## 4.0 PERFORMANCE OBJECTIVES

There were two primary objectives of this Demonstration. The first was to demonstrate the MTADS GEM-3 array (GEMTADS) on ranges away from our home location at Blossom Point. This provides a measure of system reliability and ease of use “on the road.” The second was to evaluate the probability of detection and classification ability of the combined hardware/analysis system in a blind test. A summary of the performance criteria and the resulting performance as measured during the demonstration are given in Table 1.

**Table 1. Performance objectives for the demonstration.**

Performance Objective	Metric	Data Required	Success Criteria	Results
<b>Quantitative Performance Objectives</b>				
Probability of detection	Percent detected of seeded items	<ul style="list-style-type: none"> <li>Scoring reports from ATC and Institute for Defense Analyses (IDA)</li> </ul>	$P_d=0.98$	Yes
False alarm rate	Number of false targets eliminated at a specified confidence level	<ul style="list-style-type: none"> <li>Scoring reports from ATC and IDA</li> </ul>	Reduction of false alarms by >40%	No
Sensor array SNR	Design of system such that the operating point for the system is well above the system noise floor	<ul style="list-style-type: none"> <li>Measured responses from munitions of interest (signal)</li> <li>Site background signal level (noise)</li> </ul>	$SNR \geq 10$ for all items of interest	
<b>Qualitative Performance Objectives</b>				
Reliability	Number of operational hours recorded per work day	<ul style="list-style-type: none"> <li>Field logs of operational hours per day</li> </ul>	$\geq 6/day$	Yes
Ease of use	System performs without problems and work flow is manageable for all team members	<ul style="list-style-type: none"> <li>Feedback from field team</li> </ul>	Field crew comes to work smiling	Yes
Maintenance	All required maintenance can be performed on site with available materials	<ul style="list-style-type: none"> <li>Feedback from field team on usability of technology</li> <li>Time required</li> </ul>	Minimal impact of any required maintenance on production rate	Yes

### 4.1 OBJECTIVE: PROBABILITY OF DETECTION

The combination of sensor system capability and data quality drive the probability of detection. The collection of high quality data with a capable sensor system should lead to a high probability of detecting the munitions of interest at the site.

#### 4.1.1 Metric

The metric for this objective is the percentage of seed items detected using the specified detection methodology and threshold.

### 4.1.2 Data Requirements

Scoring reports for the Standardized UXO Test Sites are provided by both the ATC and the IDA based on the prioritized dig list provided by the demonstration team.

### 4.1.3 Success Criteria

This objective will be considered to be met if at least 98% of the seeded items are detected.

### 4.1.4 Results

This objective was successfully met for munitions items buried to the U.S. Corps of Engineers (USCOE) 11-times limit. The GEMTADS surveyed the Calibration, Blind Grid, and Open Field Areas at both the APG and YPG Standardized UXO Technology Sites. For the Blind Grid Test Areas, the response stage results from Reference 11 and 13 are summarized in Tables 2 and 3, broken out by munitions size and emplacement depth. For the Open Field Areas, the response stage results from References 12 and 14 are summarized in Tables 4 and 5, broken out by munitions size and emplacement depth. The  $P_d$  is defined as the number of response-stage detections/number of emplaced munitions in the test site. The  $P_{fp}$  is defined as the (number of response stage false positives)/(number of emplaced clutter items). The probability of background alarm ( $P_{ba}$ ) is defined as the (number of response-stage background alarms)/(number of empty grid locations) for the Blind Grid. For the Open Field, the denominator is an arbitrary constant.

The GEMTADS did exhibit the ability to detect munitions at burial depths below the USCOE 11-times limit, as is discussed further in Section 8. Specifically, the Response Stage results are shown in Figure 17 (APG Blind Grid, Section 8.1.1), Figure 24 (APG Open Field, Section 8.2.1), and Figure 27 (YPG Open Field, Section 8.3.1) broken out by munitions type.

**Table 2. GEMTADS Blind Grid Test Area response stage  $P_d$  results.**

Metric	Overall	Standard	Non-standard	By Size			By depth (m)		
				Small	Medium	Large	<0.3 m	0.3 to <1 m	>=1 m
<b>APG</b>									
$P_d$	0.85	0.90	0.85	1.00	0.75	0.80	1.00	0.95	0.00
$P_d$ low 90% confidence	0.81	0.80	0.73	0.91	0.61	0.55	0.95	0.88	0.00
<b>YPG</b>									
$P_d$	0.90	0.90	0.90	0.95	0.85	0.95	1.00	0.90	0.30
$P_d$ low 90% confidence	0.85	0.83	0.78	0.86	0.69	0.75	0.95	0.79	0.08

**Table 3. GEMTADS Blind Grid Test Area response stage  $P_{fp}$  and  $P_{ba}$  results.**

Metric	Overall	By depth (m)		
		< 0.3 m	0.3 to <1 m	>=1 m
<b>APG</b>				
$P_{fp}$	0.95	0.95	0.95	1.00
$P_{fp}$ low 90% confidence	0.90	0.89	0.85	0.63
$P_{ba}$	0.20	-	-	-
<b>YPG</b>				
$P_{fp}$	1.00	1.00	1.00	N/A
$P_{fp}$ low 90% confidence	0.97	0.96	0.92	-
$P_{ba}$	0.00	-	-	-

**Table 4. GEMTADS Open Field Test Area response stage  $P_d$  results.**

Metric	Overall	Standard	Non-standard	By Size			By depth (m)		
				Small	Medium	Large	<0.3 m	0.3 to <1 m	>=1 m
<b>APG</b>									
$P_d$	0.70	0.75	0.65	0.70	0.70	0.80	0.80	0.65	0.50
$P_d$ low 90% confidence	0.68	0.71	0.60	0.65	0.62	0.71	0.77	0.61	0.44
$P_d$ upper 90% confidence	0.74	0.79	0.71	0.75	0.74	0.84	0.86	0.73	0.61
<b>YPG</b>									
$P_d$	0.80	0.80	0.80	0.80	0.75	0.90	0.80	0.80	0.50
$P_d$ low 90% confidence	0.76	0.75	0.75	0.74	0.69	0.83	0.79	0.76	0.38

**Table 5. GEMTADS Open Field Test Area response stage  $P_{fp}$  and  $P_{ba}$  results.**

Metric	Overall	By depth (m)		
		< 0.3 m	0.3 to <1 m	>=1 m
<b>APG</b>				
$P_{fp}$	0.50	0.45	0.55	0.70
$P_{fp}$ low 90% confidence	0.48	0.41	0.52	0.50
$P_{fp}$ upper 90% confidence	0.52	0.47	0.58	0.84
$P_{ba}$	0.20	-	-	-
<b>YPG</b>				
$P_{fp}$	0.80	0.80	0.80	0.30
$P_{fp}$ low 90% confidence	0.76	0.76	0.76	0.12
$P_{ba}$	0.00	-	-	-

## 4.2 OBJECTIVE: FALSE ALARM RATE

A successful anomaly classification scheme should lead to a low false alarm rate.

### 4.2.1 Metric

The false alarm rate is defined as the number of false alarms generated for some given measure, such as a survey area (#/ha). The fractional reduction in false alarms produced by using the demonstrated classification scheme as compared to using no classification scheme is the metric for success for this objective.

#### 4.2.2 Data Requirements

Scoring reports for the Standardized UXO Test Sites are provided by both the ATC and the IDA based on the prioritized dig list provided by the demonstration team.

#### 4.2.3 Success Criteria

A successful anomaly classification scheme should lead to a 40% reduction in the false alarm rate as compared to classifying all detected anomalies as hazardous.

#### 4.2.4 Results

This objective was not successfully met. The GEMTADS surveyed the Calibration, Blind Grid, and Open Field Areas at both the APG and YPG Standardized UXO Technology Sites. The results for the Blind Grid and Open Field Test Areas are summarized in Table 6 and Table 7, taken from subsections of References 11–14. Efficiency (E) and false positive rejection rate ( $R_{fp}$ ) are used to score discrimination performance ability at two specific operating points on a receiver operating characteristic (ROC) curve—one at the point where no decrease in  $P_d$  is incurred and the other at the operator-selected threshold. Efficiency is defined as the fraction of detected ordnance correctly classified as ordnance, and the false positive rejection rate is defined as the fraction of detected clutter correctly classified as clutter.

**Table 6. GEMTADS Blind Grid Test Area efficiency and rejection rates.**

	Efficiency (E)	False Positive Rejection Rate
<b>APG</b>		
At operating point	0.92	0.30
With no loss of $P_d$	1.00	0.06
<b>YPG</b>		
At operating point	0.99	0.15
With no loss of $P_d$	1.00	0.01

**Table 7. GEMTADS Open Field Test Area efficiency and rejection rates.**

	Efficiency (E)	False Positive Rejection Rate
<b>APG</b>		
At operating point	0.78	0.33
With no loss of $P_d$	1.00	0.02
<b>YPG</b>		
At operating point	0.95	0.17
With no loss of $P_d$	1.00	0.02

#### 4.3 OBJECTIVE: ARRAY SNR

To be successful, a data collection system must be designed such that at the operating point for the munitions of interest the signal level is well above the system noise floor.

### 4.3.1 Metric

The average SNR for the munitions of interest is used to evaluate this objective.

### 4.3.2 Data Requirements

To evaluate this metric, known exemplar data segments for the munitions of interest from the site and the documented system background (noise) level are required.

### 4.3.3 Success Criteria

The measured signal and background levels should produce an SNR of at least 10 for all items of interest.

### 4.3.4 Results

Given that the GEMTADS array operates with up to 10 transmit frequencies and records both in-phase and quadrature responses, there is no easy definition of SNR for this frequency domain sensor. Both the signal from UXO and the noise from several sources are a function of both frequency and in-phase/quadrature. Also at issue is the SNR level for adequate detection ( $>3$ ) versus the level for adequate discrimination ( $>10$ ).

Figure 2 plots background noise levels from various test sites surveyed by the GEM array. The top plot is the in-phase noise and the bottom plot is the quadrature noise, both as a function of transmit frequency. The black curves are from Blossom Point, the red curves from Aberdeen Proving Ground, and the green curves from Yuma Proving Ground. In-phase noise is roughly constant across frequencies but varies from two to eight ppm between the sites. Quadrature noise increases at low and high frequencies but is very quiet in the mid-frequency range ( $<1$  ppm). The various causes of these noise behaviors were reported on in a later study [6]. From a detection standpoint, mid-range quadrature signal levels of several ppm are adequate.

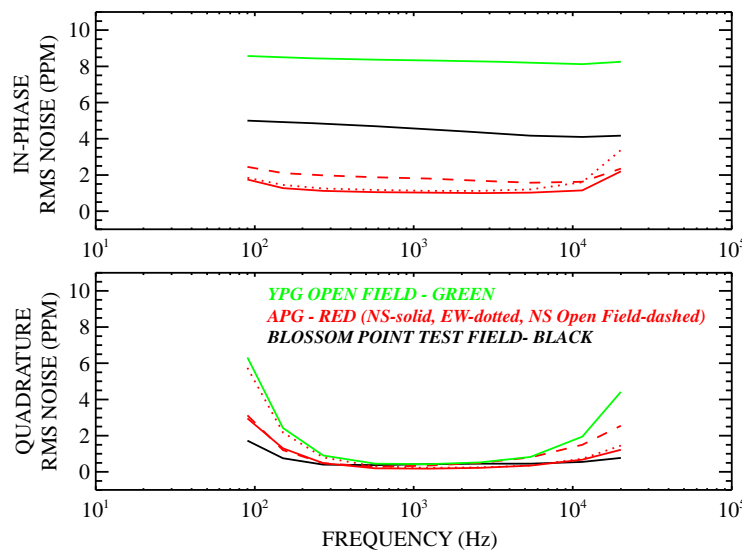


**Figure 2. GEMTADS background noise levels as measured at the three demonstration sites.**

Signal strength is driven by the magnetic polarization terms for each UXO item. These terms vary for both in-phase and quadrature as a function of frequency. For elongated UXO, there is a set for along-axis response and across-axis response. Figures 3 and 4 plot these responses for the UXO items present at the standardized test site at APG. Each plot is for a particular UXO item. There is a large degree of variation for all these items. The red curves are the quadrature response and the blue curves the in-phase response. The solid curves and dashed lines are for the along-axis and the across-axis responses, respectively. For ferrous UXO, the in-phase response changes from negative to positive across the frequency range. The quadrature response is always positive. For large ordnance, quadrature response peaks at lower frequencies and small ordnance at higher frequencies. The largest in-phase response is usually within a factor of two to four of the largest quadrature response. The across-axis response is always weaker than the along-axis response. Therefore, the average, across-axis quadrature response is considered a good indication of the weakest possible signal from an object. It is therefore a reasonable measure of SNR for the UXO targets.

Figures 5 and 6 plot the averaged over mid-frequencies, across-axis quadrature response for the APG ordnance items as a function of depth. This is the black curve in each plot. The noise level for this signal was a fraction of 1 ppm at APG. The detection SNR level ( $>3$ ) was roughly 1 ppm and the dotted red curves indicate this limit. The symbols in these plots indicate how well the GEM array performed on the Blind Grid at APG. The red X's are items that were not detected. The red symbols are plotted at the depths from the ground truth with the peak signal measured at the expected object location. In all missed item cases, the black predicted curve falls below the 1 ppm limit at the ground truth depths. These undetectable UXO items were all buried at depths greater than 11 times their diameter; most current EMI sensors would not detect these items. (This result is shown again in Section 8.1.1 and Figure 17.) From a detection stand point, the SNR levels of the GEM array are adequate.

Target discrimination with the GEM-3 array was conducted by using a model-based inversion of the polarization responses from the data and matching these responses to a library of responses for the expected UXO items. If the inverted parameters match a particular library item well, the object is identified as this type of UXO. If the parameters don't match any library item well, the item would be identified as clutter. The inverted parameters were for both in-phase and quadrature across the frequency range plotted in Figures 3 and 4. The library was made up of the responses shown in these figures with some added entries where ordnance orientation had an effect on the response (such as aluminum tail fins for an 81 mm nose down). Good inversion of the polarization parameters requires a high SNR signal—SNR levels of 10 or greater. For quadrature parameters, this criterion would be met with a signal of 10 ppm or greater on the APG site. The in-phase noise levels were greater ( $\sim 2$  ppm) and in-phase signals of 20 ppm would be required. Because the library matching looks at both in-phase and quadrature across all frequencies, there is no clear level of signal strength that predetermines good discrimination.



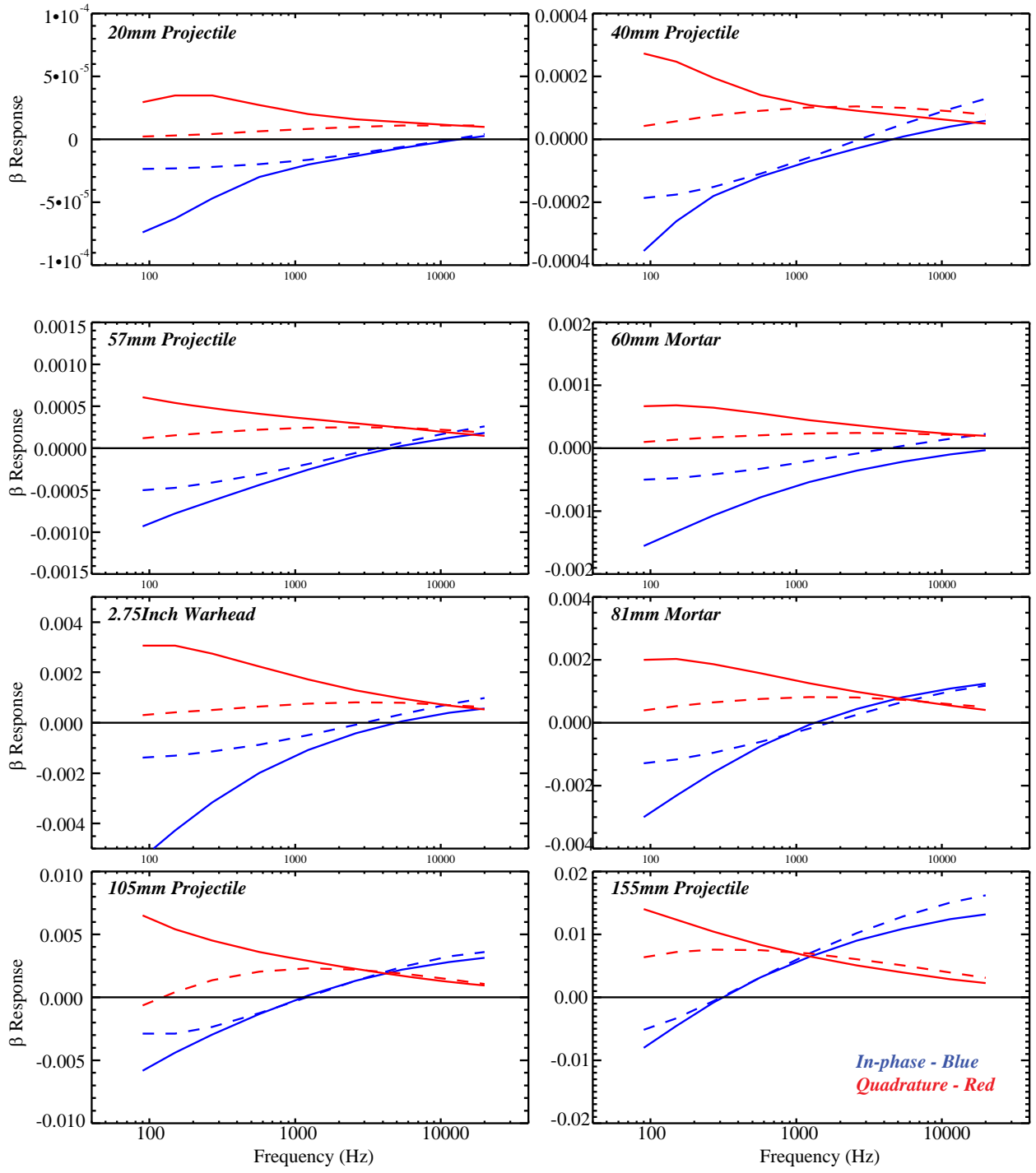


**Figure 3. In-phase (blue) and quadrature (red) response as a function of frequency for eight of the APG UXO set and the GEMTADS array.**

Along- and across-track responses are shown as solid and dashed lines, respectively.

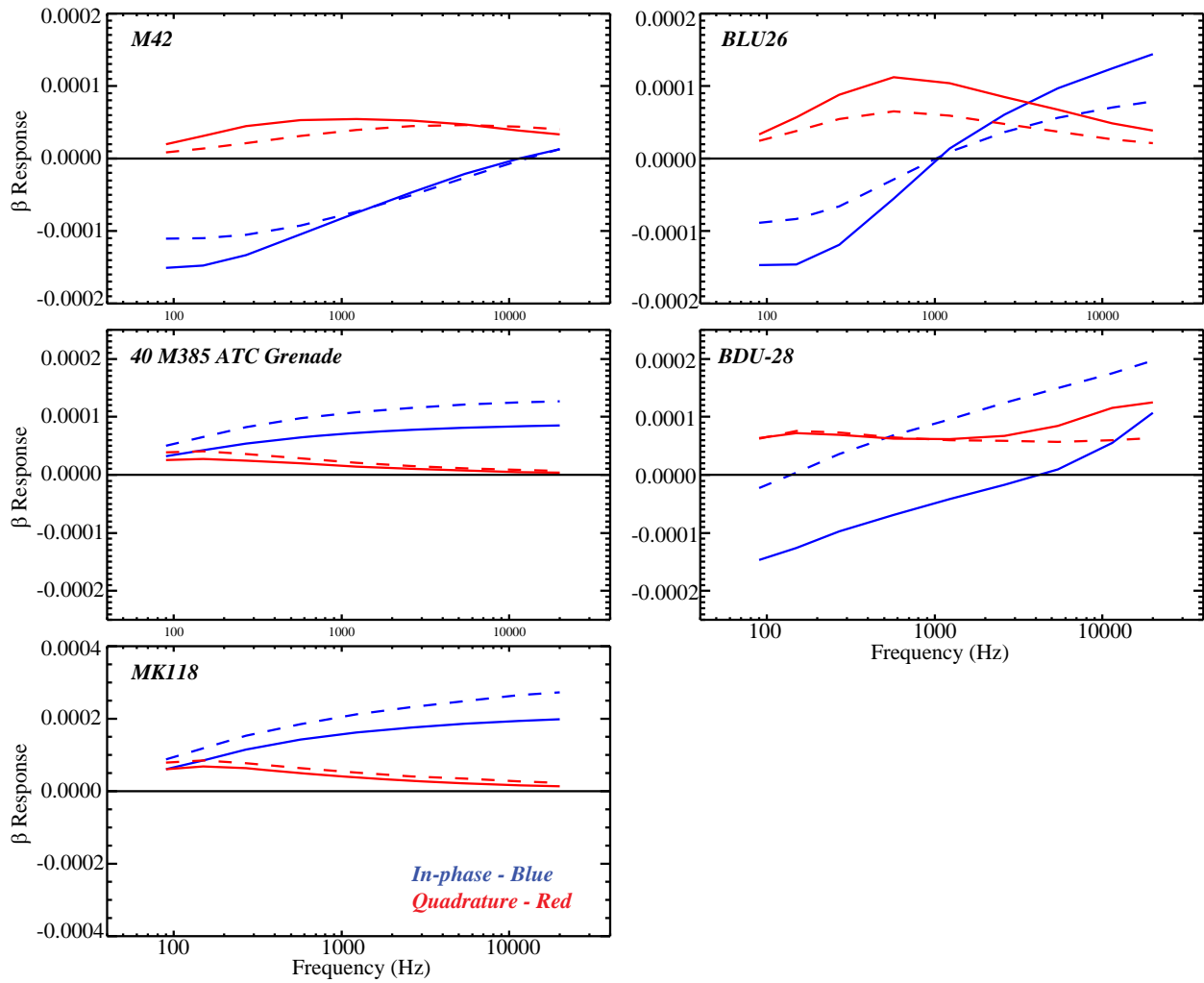


**Figure 4. In-phase (blue) and quadrature (red) response as a function of frequency for five of the APG UXO set and the GEMTADS array.**

Along- and across-track responses are shown as solid and dashed lines, respectively.

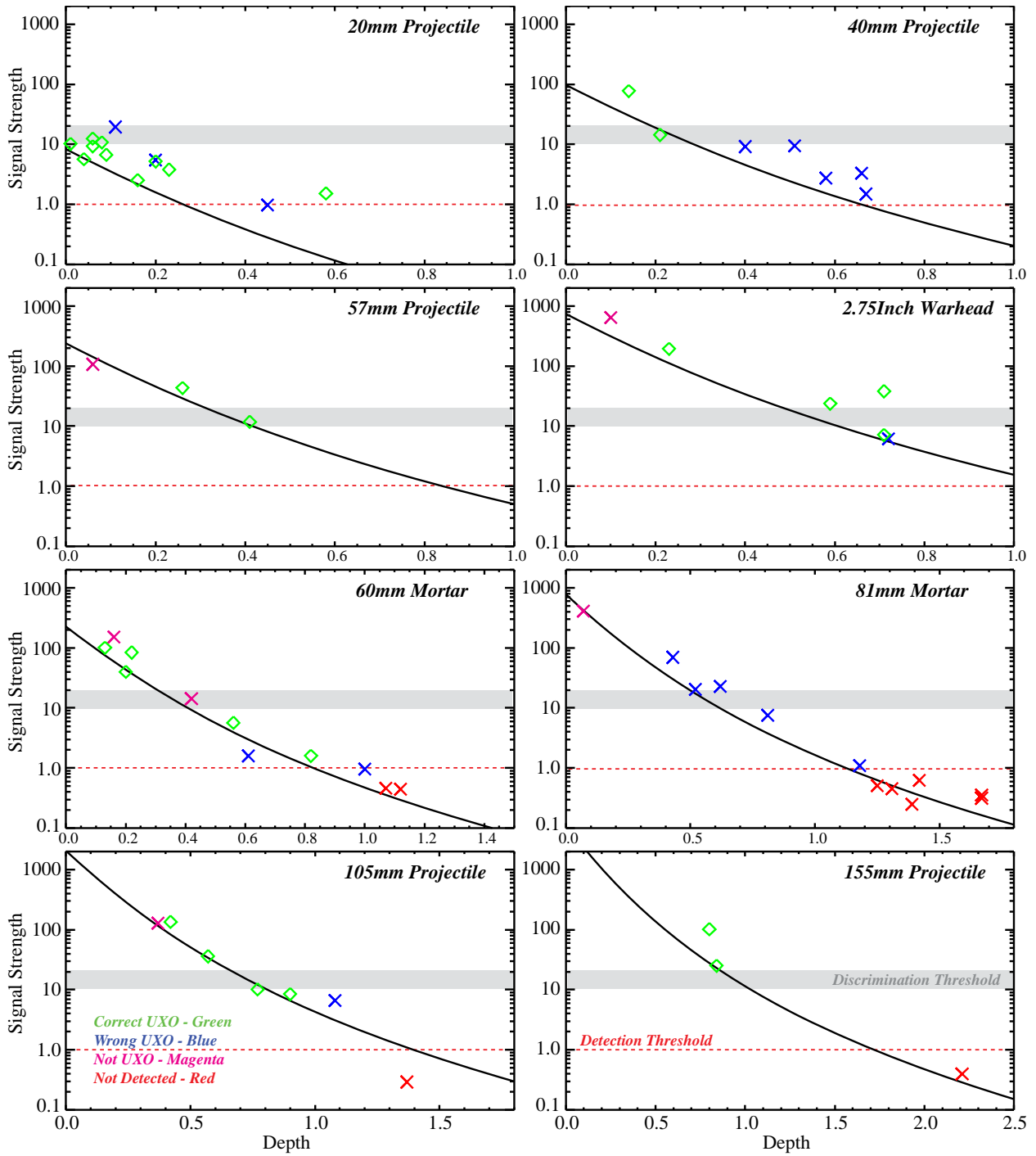


**Figure 5. GEMTADS cross-axis quadrature response, averaged over mid-frequencies for eight of the APG ordnance items as a function of depth (black curve).**

The detection SNR level is also shown (dotted red curves). The symbols indicate the GEM-3 array performance on the Blind Grid at APG.

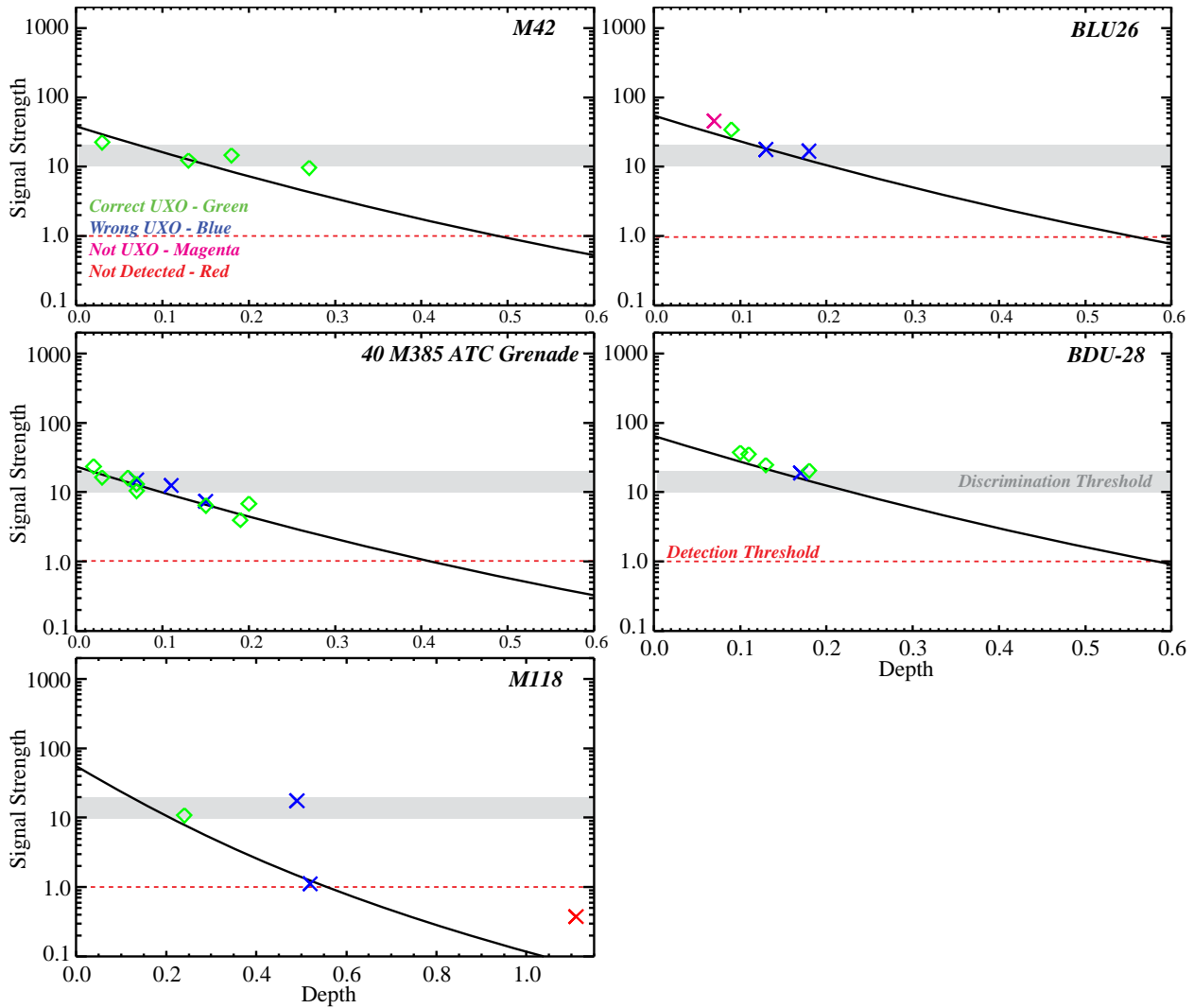


**Figure 6. GEMTADS cross-axis quadrature response, averaged over mid-frequencies for five of the APG ordnance items as a function of depth (black curve).**

The detection SNR level is also shown (dotted red curves). The symbols indicate the GEM-3 array performance on the Blind Grid at APG.

As a rough indication, Figures 5 and 6 plot the region of 10-20 ppm in gray as a discrimination threshold. Actual discrimination performance on the APG Blind Grid is plotted by the green (correctly identified UXO), blue (identified as another UXO), and magenta (UXO called clutter) symbols. Many of the ordnance items buried on the Blind Grid had signal strengths at or below the 10-20 ppm level (70%). The general trend is that these weaker UXO were incorrectly identified. While not shown, 60% of the clutter had signal strengths of less than 20 ppm. Almost all this weak clutter was incorrectly identified as UXO. Most of the strong signaled clutter was correctly flagged. The prevalence of SNR levels of less than 10 does appear to be a limiting factor in the GEM-3 array data.

There are, however, a fair number of exceptions. The 20 mms were correctly identified in the 1 to 10 ppm region. The 81 mms were flagged as UXO, but the wrong type. Most of them were identified as 2.75-inch warheads, which closely matches the 81 mm library response. Besides

SNR, another significant factor for this site is the large number of items that need to be identified and discriminated. Given the combination of low SNR and the large library to compare fitted data to, it is no surprise that the discrimination results were so poor.

#### **4.4 OBJECTIVE: RELIABILITY**

One of the main objectives of this demonstration is to collect high-quality, classification level data at survey production rates. As a base requirement to achieve this objective, the system must be capable of routinely collecting data for a full work day.

##### **4.4.1 Metric**

This metric is simply the average number of hours that the system operated each work day.

##### **4.4.2 Data Requirements**

Field records will be used to document the demonstration performance towards this objective.

##### **4.4.3 Success Criteria**

Routine survey operations of 6 hours or more per field day.

##### **4.4.4 Results**

This objective was successfully met. For full field work days (i.e., not including mobilization days), data collection was under way for at least 6 hours per day. On many days, 8-10 hours of data collection occurred.

#### **4.5 OBJECTIVE: EASE OF USE**

This objective represents an opportunity for all parties involved in the data collection process, especially the vehicle operator, to provide feedback on areas where the process could be improved.

##### **4.5.1 Metric**

The system performs without significant and unexpected problems for the field crew. Additionally, the tempo of the data preprocessing work flow is manageable for all team members.

##### **4.5.2 Data Requirements**

Discussions with the entire field team and other observations were used along with field records.

##### **4.5.3 Success Criteria**

A four-person team is able to perform all data collection and analysis tasks without a backlog developing. Additionally, the field team comes to work each day smiling.

#### **4.5.4 Results**

This objective was successfully met. The use of the four-person field team provided sufficient personnel to allow for continuous operations without undue fatigue throughout the work day by rotation of duties among the field team.

#### **4.6 OBJECTIVE: MAINTENANCE**

Field survey working conditions are hard on geophysical equipment, especially custom-modified or custom-build prototype systems that have not had the benefit of extensive field testing and hardening. On-site maintenance is a requirement. Having the tooling and equipment spares on site can shorten downtimes due to maintenance or a failure from days to minutes.

##### **4.6.1 Metric**

All routine maintenance can be performed on site with available materials.

##### **4.6.2 Data Requirements**

Discussions with the entire field team and other observations were used along with field records.

##### **4.6.3 Success Criteria**

All routine maintenance was accomplished on site, and all required spare parts were in the inventory.

##### **4.6.4 Results**

This objective was successfully met. An issue with the strain relief system for the GEM-3 cables running from the sensors to the tow vehicles was uncovered at YPG. The cabling was repaired on site to continue the survey. The issue was resolved upon return to our home facility and did not reoccur for the APG demonstration.

## **5.0 SITE DESCRIPTION**

The location of the demonstration test sites were selected by the principal investigator (PI) of the Standardized UXO Technology Test Site Program. We demonstrated this technology at both the APG and YPG sites.

### **5.1 SITE LOCATION AND HISTORY**

The area of the Aberdeen Test Site is adjacent to the Trench Warfare facility at the APG. The specific site was obviously used for a variety of ordnance tests over the years. Our initial magnetometer and EMI survey was performed after a mag-and-flag survey of the area identified more than a thousand remaining anomalies. These data were used for a final cleanup of the site prior to the establishment of the Standardized UXO Technology Site and test target emplacement.

The Yuma Test Site is located adjacent to the Mine Test Area at YPG. The area was reasonably clear before establishment of the Standardized UXO Technology Site. Our initial survey found far fewer residual anomalies after the initial clearance than was the case for the Aberdeen site.

#### **5.1.1 Climate and Weather**

During the last week in September and the first week in October, the normal high for Aberdeen is in the low 70s °F and the normal low is in the low 50s °F. Average precipitation is 0.12 inches each day. In 2003, temperatures were normal but precipitation was more than twice the long-term average. In fact, there were two tropical events in the 7 days before our survey. This rendered much of the test site too wet for a survey. We returned to Aberdeen in June 2004 to complete the survey. During this survey, temperatures were seasonal and precipitation was low. The Yuma Demonstration was performed in November 2003. During the month of November, the normal high is in the low 80s °F and the normal low is in the high 30s °F. Average precipitation is 0.2 inches for the month. The average winds are 4 mph. During the period of our survey, temperatures were normal but we again experienced an unusual rain event. This caused a one-day delay in starting the survey but did not affect our performance otherwise.

#### **5.1.2 Topography**

The portions of the Aberdeen site covered in this demonstration (the Calibration Lanes, Blind Test Grid, and Open Field) are relatively flat and level. There are some low-lying areas in the northwest portion of the Open Field area that tend to have standing water during wet periods of the year. We were able to survey through this standing water with the MTADS magnetometer system but would not have been able to take the GEM-3 array through water of such depth. As it turned out, the standing water was much worse during our first visit. In June 2004, the water was again at normal levels.

The scenarios at the Yuma site that were covered in this demonstration (the Calibration Lanes, Blind Test Grid, and Open Field) are also relatively flat and level. Due to the presence of washes and scattered trees on the Open Field site, we were not able to cover every square meter of the site with the vehicular towed system. We surveyed along the edge of the washes on both sides

and then down in them as was feasible. The coverage we achieved in the Open Field site was representative of vehicle-towed systems.

### 5.1.3 Site Maps and Photographs

An aerial photograph of the Aberdeen test site is shown in Figure 7. The various scenarios are outlined and numbered. The scenarios of concern here are the Calibration Lanes (1) and Blind Test Grid (2) outlined in blue and the Open Field (3) outlined in yellow. We did not survey either the mogul (4) or wooded (5) areas.



**Figure 7. Aerial photograph of the Aberdeen Test Site with the various scenarios outlined.**

A corresponding aerial photograph of the Yuma test site is shown in Figure 8. The various scenarios are outlined. The scenarios of concern here are the Calibration Lanes, the Blind Test Grid, and the Open Field. We did not survey either the mogul or Yuma Desert Brush areas.



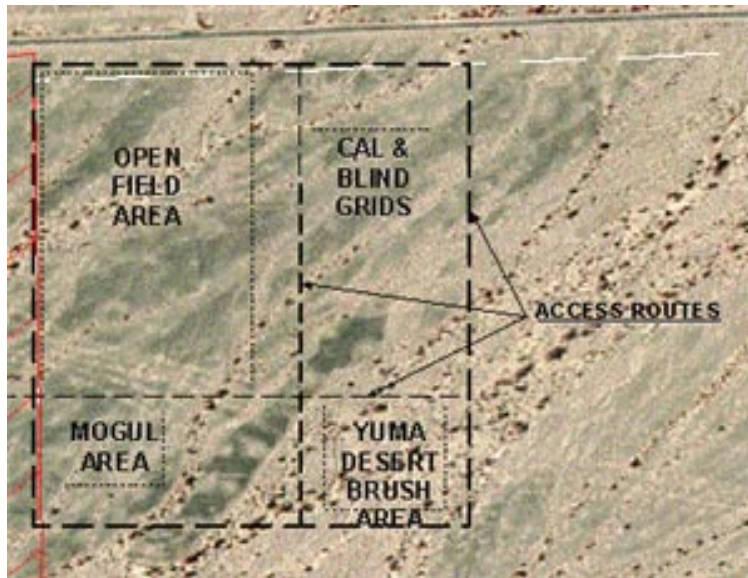


**Figure 8. Aerial photograph of the Yuma Test Site with the various scenarios outlined.**

## **5.2 MUNITIONS CONTAMINATION**

The APG and YPG Standardized UXO Technology Sites were seeded with a variety of munitions and submunitions by the PIs of the sites from the ATC Standardized Target Repository [7]. The included munitions types span a large range of sizes and material compositions. They include small projectiles (20 mm M55, 25 mm M792, 37 mm M63M1, 40 mm MkII, and 57 mm M86), submunitions (M42, BDU-26, and BDU-28), medium mortars (60 mm M49A3 and 81 mm M374), and large projectiles (105 mm M456 HEAT, 105 mm M60, and 155 mm M483A1). A variety of clutter has also been seeded within the sites.

*This page left blank intentionally.*

## 6.0 TEST DESIGN

### 6.1 CONCEPTUAL EXPERIMENTAL DESIGN

The demonstration was designed to be executed in two stages. During the first stage the GEMTADS sensor array, as demonstrated, was characterized with respect to the items of interest. Measurements of example munition articles of interest were made to generate library signatures for use during the data analysis and classification process.

The second stage of the demonstration consisted of surveys of the APG and YPG Standardized UXO Technology Sites using the GEMTADS. The Calibration and Blind Grid areas at each site were surveyed. For each site, the surveyable portion of the Open Field scenario was surveyed as well. Each data set was then inverted using the data analysis methodology discussed in Section 7.3, and estimated target parameters determined. These target parameters were then used to classify each detected anomaly as described in Section 7.4. The results are discussed at length in Reference [8].

The schedule of field testing activities is provided in Figure 9 as a Gantt chart.

Activity Name	2003				2004					
	Sept	Oct	Nov	Dec	Jan	Feb	Mar	Apr	May	Jun
GEMTADS Demonstrations	[Blue bar spanning Sept 2003 to June 2004]									
APG Data Collection - Part I	[Blue bar spanning Sept to Oct 2003]									
APG Data Collection - Part II										[Blue bar in Jun 2004]
YPG Data Collection			[Blue bar in Nov 2003]							
	Sept	Oct	Nov	Dec	Jan	Feb	Mar	Apr	May	Jun

**Figure 9. Schedule of field testing activities.**

### 6.2 SITE PREPARATION

As the APG and YPG Standardized UXO Technology Sites are established sites with logistics in place, no additional site preparation was required.

### 6.3 SYSTEMS SPECIFICATION

This demonstration was conducted using the NRL MTADS tow vehicle and subsystems. The tow vehicle and each subsystem are described further in the following sections.

#### 6.3.1 MTADS Tow Vehicle

The MTADS has been developed by the NRL Chemistry Division with support from ESTCP. The MTADS hardware consists of a low-magnetic-signature vehicle that is used to tow the different sensor arrays over large areas (10–25 acres/day) to detect buried UXO. The MTADS tow vehicle and GEM-3 array are shown in Figure 10.



**Figure 10. MTADS GEM-3 array in operation pulled by the MTADS tow vehicle.**

### **6.3.2 GEM-3 (GEMTADS) Array**

As discussed in Section 3.1, the MTADS GEM-3 array consists of three, 96-cm diameter GEM-3 sensors (Geophex, Ltd.) in a triangular configuration with two sensors across the front of the array and one centered in the rear. The nominal ride height of the sensors is 33.5 cm above the ground. The roughly 2-m square array is shown schematically in Figure 11. Figures 1 and 10 show the configured array being pulled by the MTADS tow vehicle. The sensors have been false-colored (red, green, blue) in Figure 1 to match the color scheme used in the other figures in this report and in the Data Acquisition (DAQ) system software display. The array is mounted on a rigid support that is attached to the MTADS electromagnetic (EM) trailer using non-metallic fasteners.

Individual sensors in the array are located using a three-receiver real time kinematic (RTK) GPS system shown schematically in Figure 11 [9]. The three-receiver configuration extends the concept of RTK operations from that of a fixed base station and a moving rover to moving base stations and moving rovers. The lead GPS antenna (and receiver, MB1) receive corrections from the fixed base station at 1 Hz. This corrected position is reported at 10-20 Hz using a vendor-specific National Marine Electronics Association (NMEA) NMEA-0183 message format (PTNL,GGK or GGK). The MB1 receiver also operates as a “moving base,” transmitting corrections (by serial cable) to the next GPS receiver (MB2), which uses the corrections to operate in RTK mode.

A vector (AVR1, heading [yaw], angle [pitch], and range) between the two antennae is reported at 10 Hz using a vendor-specific NMEA-0183 message format (PTNL,AVR or AVR). MB2 also provides “moving base” corrections to the third GPS antenna (MR), and a second vector (AVR2) is reported at 10 Hz. All GPS measurements are recorded at full RTK precision, ~2-5 cm. All sensor readings are referenced to the GPS 1-PPS output to fully take advantage of the precision of the GPS measurements. An IMU is also included on the sensor array to provide complementary platform orientation information. The IMU is a Crossbow VG600 running at approximately 83 Hz.

A close-up view of the sensor platform is shown in Figure 1, which shows the three GPS antennae and the IMU (black box under the aft port GPS antenna). The airborne adjunct of the MTADS, the Airborne Multisensor Towed Array Detection System (AMTADS) uses a similar configuration with two GPS antennae/receivers to provide the yaw and roll angles of the sensor boom and pitch from the IMU [10].

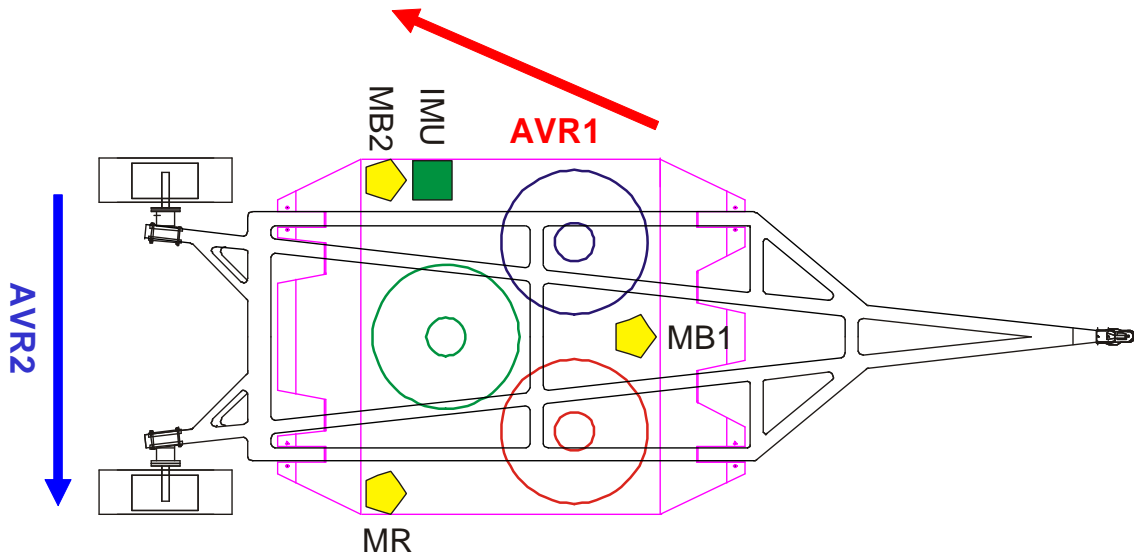


**Figure 11. MTADS EM trailer with approximate locations of GPS and IMU equipment indicated.**

The colored circles represent the GEM-3 sensors of the GEMTADS array.

The standard GEM-3 sensor drive electronics have been modified to produce a substantially higher transmit moment for this array. Each individual sensor can transmit a composite waveform of one to 10 frequencies in the frequency range of 30 to 20,010 Hz with a base period of 1/30 s. For this survey, a composite transmitter waveform of nine frequencies log-spaced from 90 to 20,010 Hz is used. Two additional base periods are required for signal deconvolution and to output the response from each sensor. The array can therefore operate continuously with one sensor actively transmitting while the other two sensors are processing data at any given time. Allowing for a short coil settling time between the transmissions from each sensor, an effective array sampling rate of just over 9 Hz is achieved. Sequential transmitter operation also alleviates the need for the orthogonal survey mode employed for the EM61 MkII array. Coupled with our standard survey speed of 3 mph, the result is a down-track sampling spacing of ~15 cm with a cross-track spacing of 50 cm. An interleaved survey pattern is used to decrease the cross-track spacing to 25 cm as depicted in Figure 12.

The GEM-3 sensors are controlled by a custom electronics package designed and built by Geophex, Ltd. It is mounted in an equipment rack in the MTADS tow vehicle as shown in Figure 13. Overall control of data collection is accomplished with a custom version of the standard GEM-3 sensor control software, WinGem2KArr, running under Windows 2000 on our data acquisition computer. An example of the working screen of this program is shown in Figure 14. This software package logs the data from the GEM-3 sensors, the three GPS NMEA sentences, the time of the GPS 1-PPS pulse, the GPS Universal Coordinated Time (UTC) time stamp, and the IMU data in separate files with a common base survey name. The data are periodically transferred to the data analyst for immediate QC checks and for further processing.

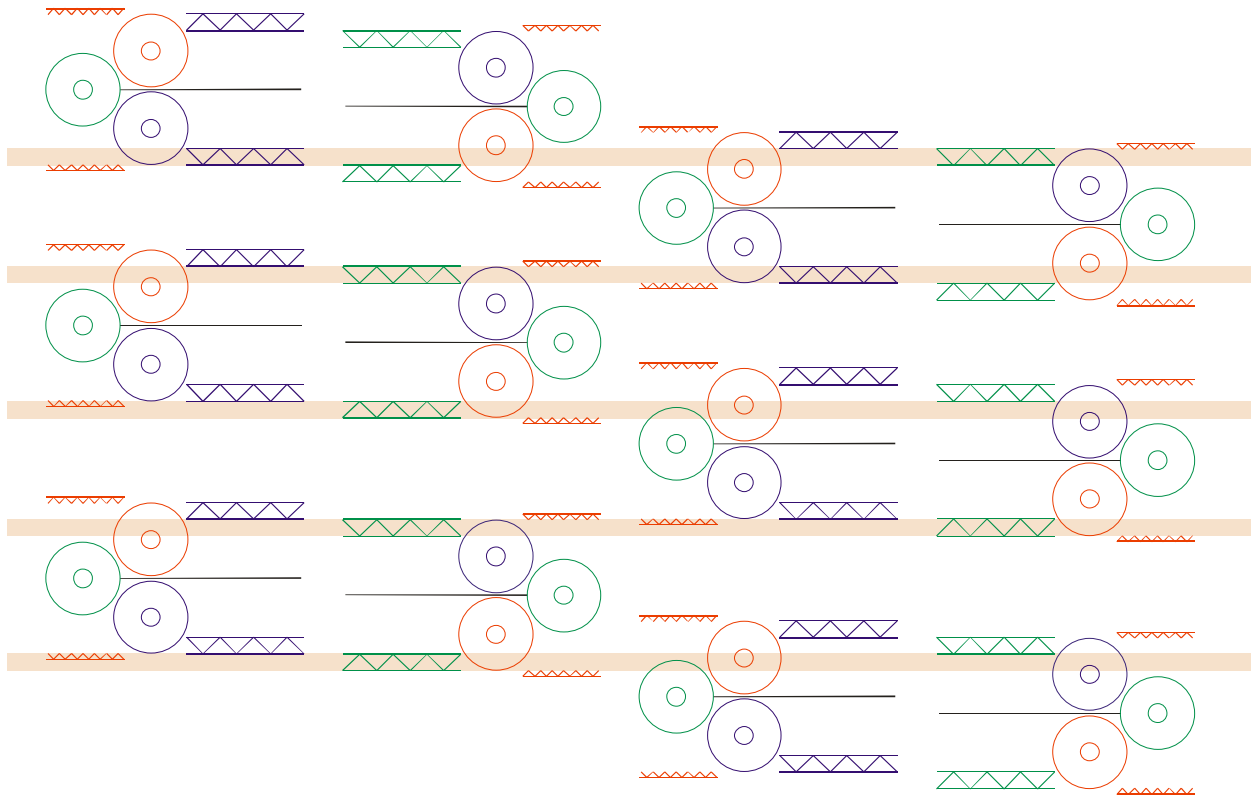


**Figure 12. Schematic of interleaved survey pattern for GEMTADS surveys.**  
 The sensors are depicted as colored circles. The large crosshatched sections indicate the path of the tow vehicle tires. The outer extents of the swath of the EM trailer tires are represented by the narrow crosshatching. The tan bars represent areas where two tire tracks are collocated.



**Figure 13. GEM-3 array control electronics and GPS receivers.**

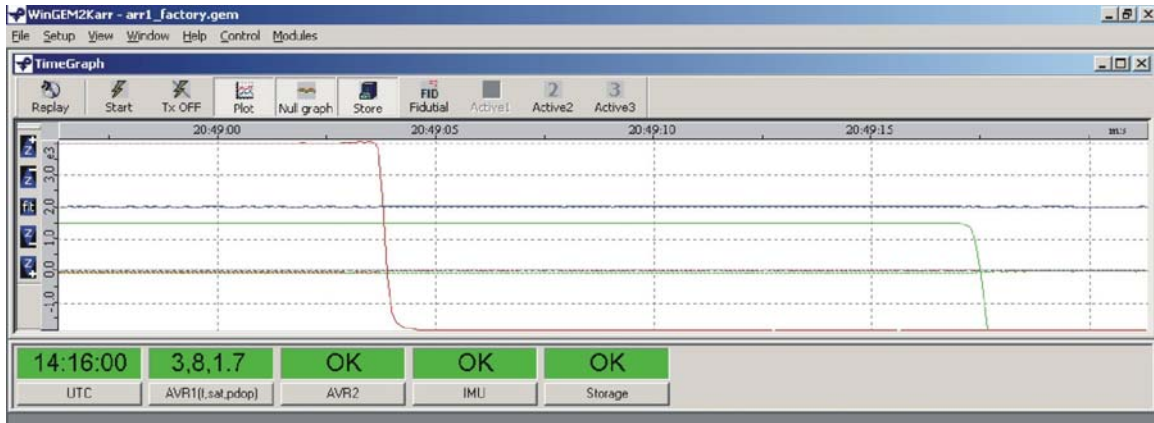


**Figure 14. Working screen of the WinGEM2kArr program.**

## 6.4 DATA COLLECTION

### 6.4.1 Scale of Demonstration

The GEMTADS array was deployed to the APG and YPG Standardized UXO Technology Sites in Fall 2003 and Spring 2004 for APG, and Winter 2003 for YPG. The areas of the surveyed portions of the two Standardized UXO Technology Sites and the coverage achieved by GEMTADS array for each area are detailed in Table 8. Each data set was then inverted using the data analysis methodology discussed in Section 7.3, and estimated target parameters determined. These target parameters were then used to classify each detected anomaly as described in Section 6.5.

**Table 8. Survey coverage of GEMTADS array at the two test sites.**

Site	Scenario	Area (ha)	GEMTADS Array Coverage (ha)	Fraction
Aberdeen	Calibration Lanes	0.12	0.12	100%
	Blind Grid	0.19	0.19	100%
	Open Field	5.54	4.89	88%
Yuma	Calibration Lanes	0.11	0.11	100%
	Blind Grid	0.17	0.17	100%
	Open Field	6.23	5.92	95%

### 6.4.2 Sample Density

Based on our standard survey speed of 3 mph, a down-track sampling spacing of ~15 cm, and a cross-track spacing of 50 cm, the expected data density is 14 points per m<sup>2</sup>. With the interleaved survey pattern, this doubles to 28 points per m<sup>2</sup>. See Section 6.3.2 for further details.

### 6.4.3 Quality Checks

The following procedure constitutes a typical startup for the MTADS system for both initial startup and as daily system evaluations. The RTK GPS base station receiver and radio link are established on a previously established control point. The validity of the control point location will be verified using the MTADS man-portable RTK GPS rover receiver to occupy one or more

of the established control points using the control point occupied by the GPS base station as a reference.

The standard performance checks include three types of measurements. Initial system startup, at the beginning of field work and again each morning, consists of three measurements. First, quiet, static data are collected for a period of 15-20 minutes with all systems powered up and warmed up (typically 30 minutes). Next, two calibration items, a 4-inch diameter aluminum (Al) sphere and a ferrite rod bundle, are placed a standard distance above the center of each sensor coil several times in sequence to verify the response of each sensor to each object. The system is stationary for this data collection. Finally, a systems timing check using a fixed-position wire or chain placed on the ground is conducted. At the discretion of the PI, the timing check may be repeated in the middle of the survey day. At the discretion of the PI, the timing check and the Al sphere and ferrite measurements may be repeated at the end of the day.

The data quality checks conducted on each data set are discussed in Section 7.1.

#### **6.4.4 Data Summary**

The primary performance metrics of this demonstration are the detection and discrimination performance of the GEMTADS array at the two Standardized UXO Technology Demonstration Test Sites. These results are provided by the site managers after detection and discrimination picks are submitted [11-14, 12, 13, 14]. The ground truth of these sites is held by the PIs and results are only reported in aggregate.

### **6.5 VALIDATION**

With the exception of the Calibration Grid, the ground truth for the Standardized sites is held back from individual technology demonstrators to preserve the utility of the Blind Grid and Open Field Areas. Results from the Blind Grid and the Open Field Area were submitted to ATC for performance evaluation. Scoring results have been received and are available [11-14]. A summary of the results is given in Section 8.



## 7.0 DATA ANALYSIS AND PRODUCTS

### 7.1 PREPROCESSING

The processing steps necessary to consolidate the individual raw data files recorded by the data acquisition computer (refer to Section 6.3.2) to a product feasible for analysis are coarsely outlined in the block diagram of Figure 15.

Corrections based on recent or same day ferrite measurements are first applied to each of the three GEM-3 data files. In theory, the frequency response to ferrite should be flat and negative for the in-phase, and zero for the quadrature. Amplitude and phase corrections based on this are therefore applied to correct for and equalize the response of all three GEM-3 sensors. In addition, a running median window is subtracted from each of the GEM-3 time series (on a per frequency basis) to mitigate sensor drift—a problem especially at the higher frequencies. A window width of 500 points (~50 s) was chosen for both the APG and YPG Open Field GEM-3 data.

As described in Section 6.3.2, the GPS data files contain NMEA GGK sentences yielding the position of the master antenna (MB1 in Figure 11) at 20 Hz, as well as AVR sentences yielding the vectors to the other two antennae (represented by the red and blue arrows in Figure 11) at 10 Hz. These vectors are defined by their magnitudes (range) and two angles (yaw and tilt), with the yaw angle defined relative to true north. By first redefining the yaw angle to be relative to grid north, the along-platform and cross-platform vectors are subsequently computed from the two AVR vectors allowing the pitch and roll angles of the platform to be readily determined. Because all sensors are mounted on the same rigid board, the orientation of all the sensors is now completely determined.

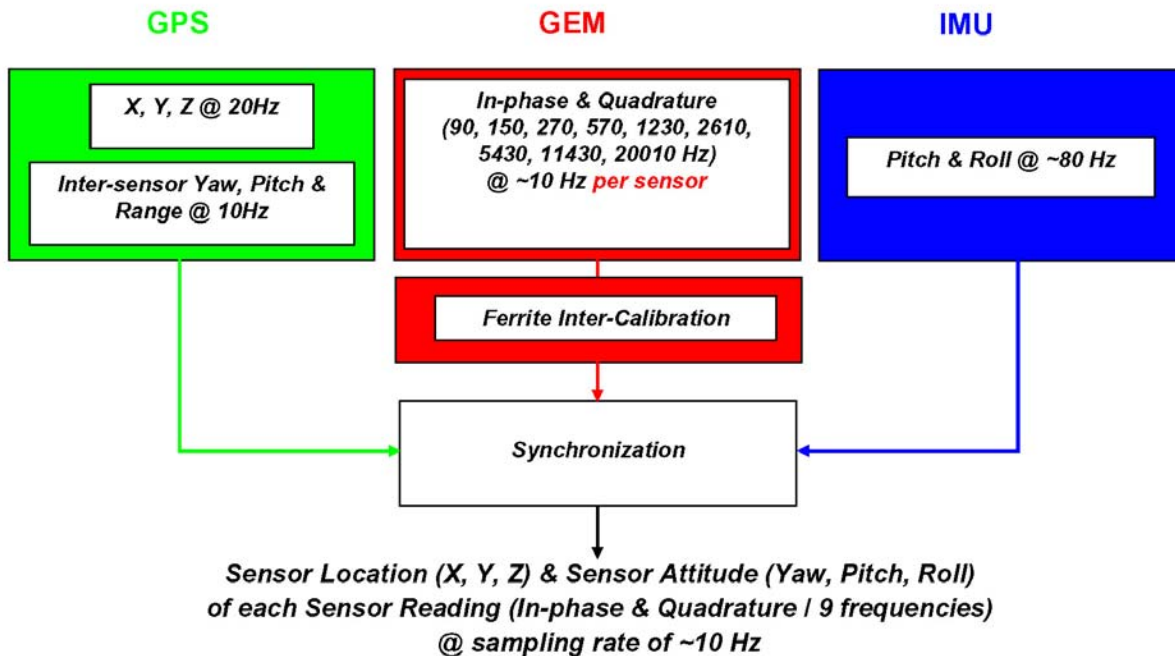


**Figure 15.** A schematic diagram showing the integration of the GEM and navigation data for eventual analysis.

To perform the final integration of data, all sensors need to be synchronized. As discussed in Section 6.3.2, this is mostly taken care of in the data acquisition phase by referencing all data to the GPS 1-PPS, with an added sensor latency determined by driving the array back and forth over a metal pipe. Since this latter latency tends to change unpredictably over time, it is necessary to perform such a measurement on a continual basis. On implementation of this latency, the location and orientation—a combination of the IMU and GPS pitch and roll (Section 6.3.2)—of each GEM sensor at a given time is matched to a given spectrum.

## 7.2 TARGET SELECTION FOR DETECTION

The process of anomaly identification, or detection, from the survey data was done using the  $Q_{avg}$  quantity, the average of the quadrature response for the middle five frequencies.

$$Q_{avg} = \frac{\sum(Q_{270Hz} + Q_{570Hz} + Q_{1230Hz} + Q_{2610Hz} + Q_{5430Hz})}{5}$$

We chose this metric because of the lower noise in the quadrature response and the good signal in the mid frequencies for the objects of interest. The performance of this metric on the APG and YPG data sets is discussed in Sections 8.1.1 (APG Blind Grid), 8.2.1 (APG Open Field), and 7.3.1 (YPG Open Field) respectively.

## 7.3 PARAMETER ESTIMATES

The located demedianed GEMTADS data (position, orientation, and nine data pairs (in-phase and quadrature response for nine transmit frequencies)) surrounding the center of each selected anomaly are extracted and submitted to a solver engine developed by Science Applications International Corporation (SAIC) for the analysis of the GEMTADS data using a standard dipole model. The solver algorithm finds six fitted parameters— $x$ ,  $y$ ,  $z$ ,  $\phi$ ,  $\theta$ ,  $\psi$ —where  $x$ ,  $y$ ,  $z$  are the target coordinates (m) and  $\phi$ ,  $\theta$ ,  $\psi$  are the Euler angles (deg) of the model output. The associated best-fit betas (set of three  $\beta$ s at each frequency for in-phase and quadrature), chi-squared ( $\chi^2$ ), and coherence are also found as part of the inversion. The betas are the principal components of the induced magnetization tensor. The  $\chi^2$  and coherence are measures of the quality of the inversion result with respect to the original source data. Follow-on fits are made while constraining the three  $\beta$ s to match appropriate given values from a library containing values for items including the items of interest. The associated  $\chi^2$  and coherence values are found for the fit to each library item, and the ratios of (constrained library fit)/(unconstrained library fit) for both  $\chi^2$  and coherence are calculated.

For each anomaly processed in the described manner, all fitted results are reported, including position ( $x,y,z$ ), orientation (three angles), polarizability spectra,  $\chi^2$  error, the correlation coefficient between model and measured data, and a signal strength metric. Both unconstrained and library-constrained inversions are performed, assuming that representative spectra are observed for certain classes of objects (such as the UXO targets of interest or unique clutter classes). The size of an equivalent sphere is also estimated from the  $\beta$ s via established parametric models.

## **7.4 CLASSIFIER AND TRAINING**

The prescription for discrimination using GEMTADS is to compare the measured response of a target to each of a set of library response functions in turn and to determine which library item results in the closest match to the target. If the match is good enough, we can declare the target as being that member of the library. To quantify the “goodness-of-fit” to this, we compute the  $\chi^2$  for the each match. Further details on the system performance are given in Section 8.1.2.

## **7.5 DATA PRODUCTS**

The primary data products generated are the ranked dig lists submitted to the site managers for scoring. Additionally, the archival data sets, stored individually by site and by area are provided for future data analysis/classification efforts.

*This page left blank intentionally.*

## 8.0 PERFORMANCE ASSESSMENT

The project objective was to demonstrate the optimum system built around the Geophex GEM-3 EMI sensor that delivers the most classification performance while retaining acceptable survey efficiency. A three-sensor array system was designed around a modified GEM-3 sensor. The system was built and characterized and then demonstrated at the Standardized UXO Demonstration sites at APG and YPG. At each of the sites, the Calibration Lanes, the Blind Test Grid, and as much of the Open Field Area as was possible were surveyed. For the Blind Test Grid and the Open Field, the ranked target picks were submitted to ATC for scoring. These scoring results are the basis for characterizing the success of the demonstrations and the performance of the array. Portions of Reference 8 are reproduced here to summarize the performance of the system.

### 8.1 ABERDEEN PROVING GROUND BLIND GRID

#### 8.1.1 Response Stage

The first stage of scoring at the Test Sites is the Response Stage where anomalies are identified or detected. For this, we use the  $Q_{avg}$  quantity, as discussed in Section 7.2. A  $Q_{avg}$  plot for the APG Blind Grid is shown in Figure 16. The 400 cells in the Blind Grid are marked with white squares in Figure 16. A summary of the GEMTADS array detection performance is given in Table 9.

**Table 9. Summary of detection performance at the APG Blind Grid.**

Cell Contents	Number of Cells	Number Correct	Number Incorrect
Single ordnance item	84	73	11
Ordnance item with clutter	7	7	0
Single clutter item	95	91	4
Two clutter items	8	8	0
“Empty”	206	174	32
Total	400		

The 32 cells reported as “Empty” but for which we made a declaration require some discussion. Only 12 of these false positives showed signal in the GEM array survey only. Seven of these cells had a detection by the GEM array, the EM61 HH, and the magnetometer array. Ten had a detection by the GEM array and the EM61 HH, and three had a detection by the GEM array and the magnetometer array. An example of this is cell B8, which is highlighted in Figure 16. It is difficult to understand the observed signal unless there is some inadvertent metal in this cell.

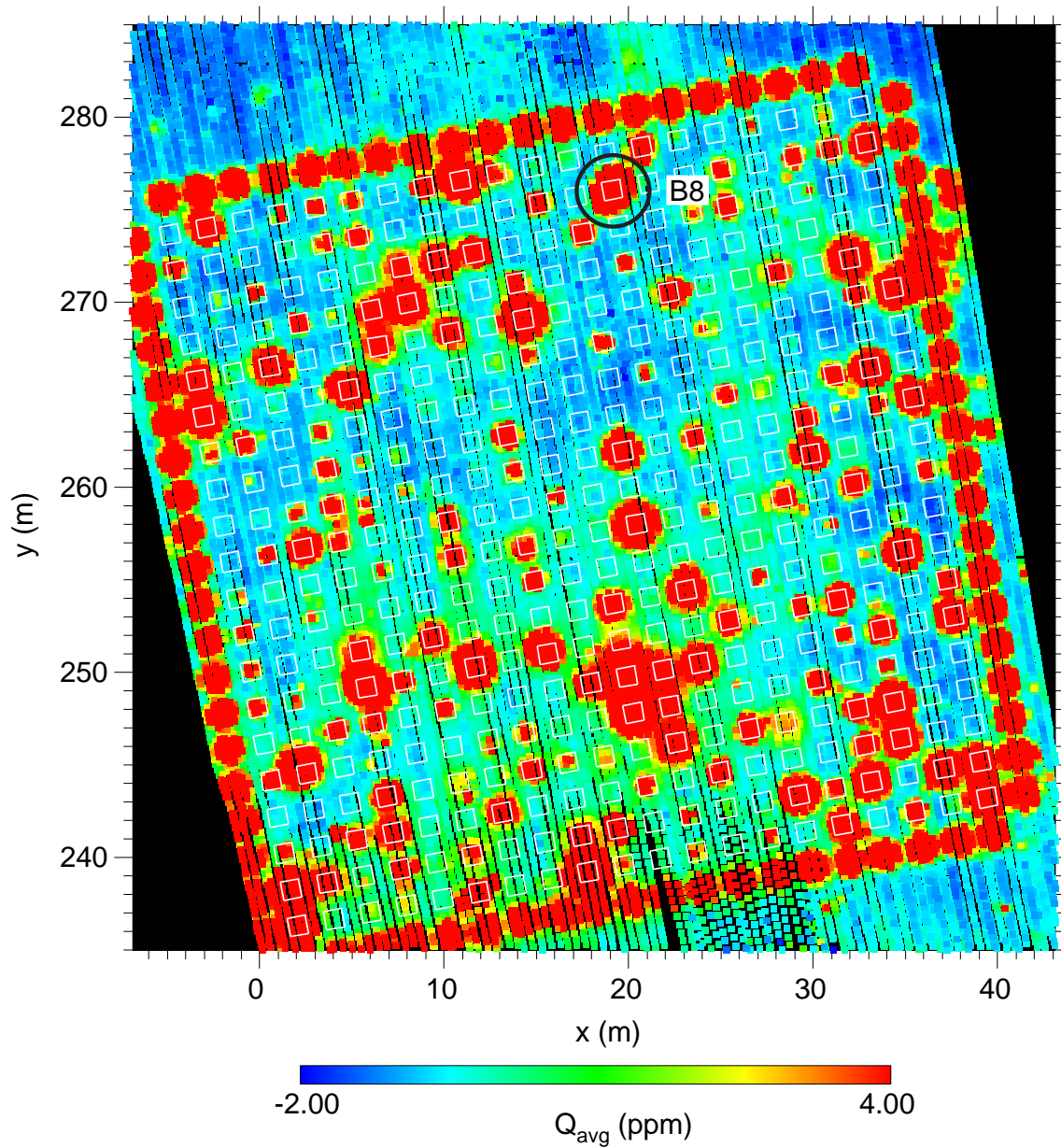


**Figure 16.  $Q_{avg}$  anomaly image map of the APG Blind Grid.**

An indication of the depth performance of the system is shown in Figure 17. The detected items are shown as black triangles and the missed items are shown as red crosses. The reference line corresponds to a depth of 11-times the item diameter. As can be seen, the GEM array is capable of detecting targets down to and below 11 times their diameter at this site.

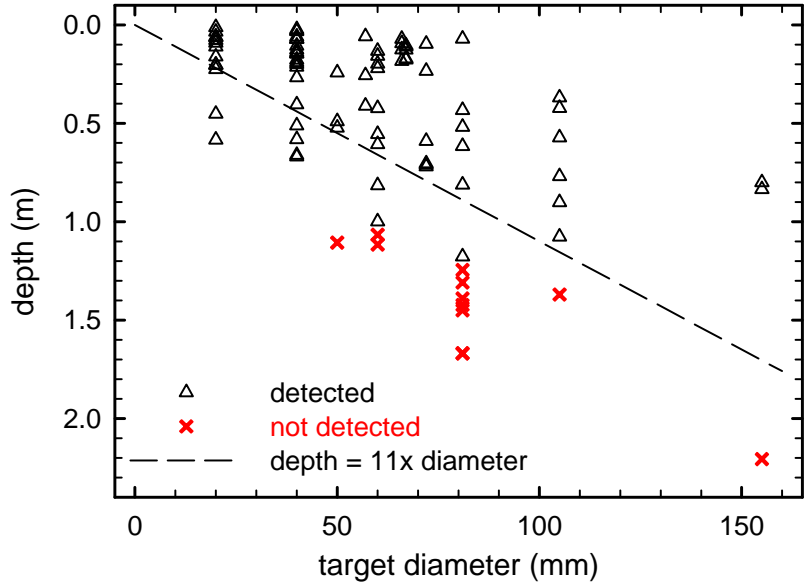


**Figure 17.  $Q_{avg}$  detection performance as a function of depth at the APG Blind Grid.**

The response stage data are plotted in Figures 18 and 19 in the manner of the Standardized Test Site scoring reports. Figure 18 shows cumulative ordnance count versus cumulative clutter count. Since the targets are ordered by signal amplitude at the response stage, it is no surprise that this plot is essentially along the diagonal.

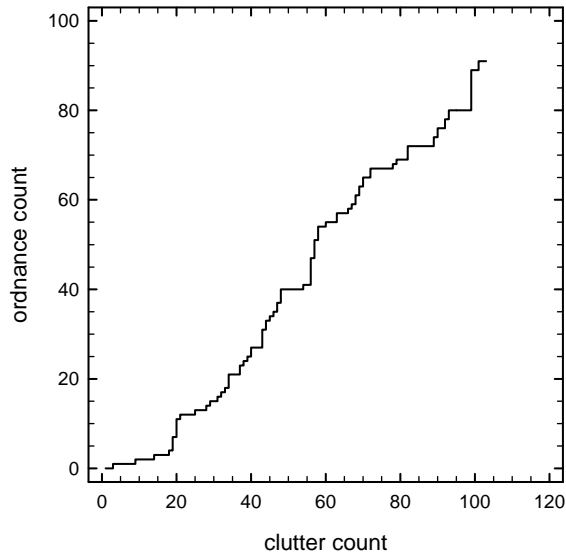


**Figure 18. Response stage results showing cumulative ordnance count versus cumulative clutter.**

A better measure of system capability is shown in Figure 19, which plots cumulative occupied cells versus adjusted cumulative blank cells. Cells such as B8, which obviously contain buried metal, were excluded from the blank count.

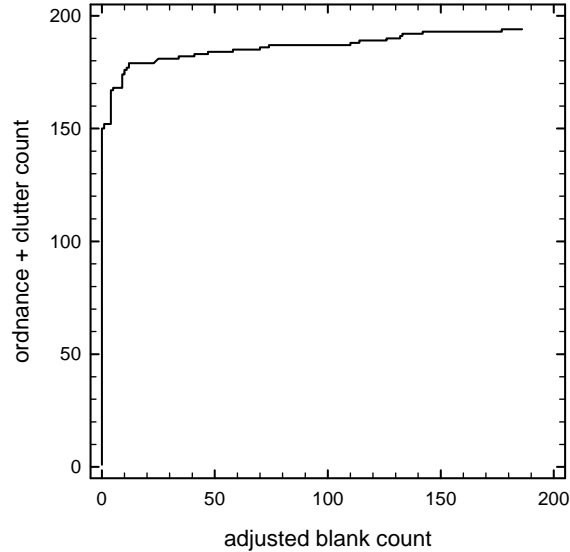


**Figure 19. Response stage performance showing cumulative occupied cell count plotted versus adjusted cumulative blank cell count.**

### 8.1.2 Discrimination Stage

Discrimination using GEMTADS is accomplished by comparing the measured response of a target to each of a set of library response functions in turn and determining which library item results in the closest match to the target. If the match is good enough, we can declare the target as being that member of the library. To quantify the goodness-of-fit, we compute the  $\chi^2$  for each match. For the APG Blind Grid, three different methods of discrimination based on the  $\chi^2$  were evaluated.

The first method is one based on the weighing of the  $\chi^2$  by the signal amplitude. If the signal level for the various targets differs by a large amount (some targets are quite shallow and some very deep) the computed  $\chi^2$  can be strongly affected by the signal amplitude. To test this possibility, we computed the  $\chi^2$  for the best match weighting the data by the usual  $1/\text{rms}^2$  (where the root mean square [rms] deviation is determined from areas between targets) and by  $1/(\text{rms} + 0.01 \times \text{signal})$  in an attempt to reduce the influence of signal amplitude on the computed  $\chi^2$ . The  $\chi^2$  calculated with the signal-based weighting was used for our declarations at the APG Blind Grid. Based on the results from the Calibration Lanes (which was all we had available at the time), we established an  $\chi^2$  threshold of 0.01 for the ordnance/clutter decisions. This is a little less than three standard deviations above the ordnance mean. The reported Discrimination Response Factor was just the inverse of the  $\chi^2$ .

The second method assumes that this strong variation of  $\chi^2$  with signal amplitude arises from the bouncing motion of the sensor array as it traverses the rough field. Over a high-signal target, small variations in  $z$  result in relatively large variations in signal as compared to over a deep, low-signal target. In this case, we can model the bouncing noise by  $(K * \text{signal})$ , and the correct weighting would be  $1/(\text{rms}^2 + (K * \text{signal})^2)$ . Based on data collected on the Blossom Point Test Field, at values of  $K$  around 0.3, the scaling of  $\chi^2$  with signal amplitude seems to flatten out.



Scaling the weights by the signal improves the performance of the discrimination but is not very practical as the scaling coefficient is determined after the fact. For the later YPG and APG Open Field demonstrations, we employed another method to mitigate the effects of bouncing noise. Each target was fit using a full, unconstrained 3- $\beta$  model as well as the library model. The ratio of the  $\chi^2$  for these two methods, which eliminates the dependence on signal amplitude, should approach 1 if the item is in the library.

The ROC curves for the application of these three discrimination methods to the APG Blind Grid are shown in Figures 20 through 22. The standard  $\chi^2$  weighting (Figure 20) and the modified weighting with “bounce noise” added (Figure 21) result in curves that vary little from the chance diagonal. There are fewer items in Figure 21 than in Figure 20. The original submission to APG required that a discrimination score be included for all cells, even those below our detection threshold. We arbitrarily assigned these cells a low discrimination score. The  $\chi^2$  with “bouncing noise” analysis was applied only to cells in which we declared a detection.

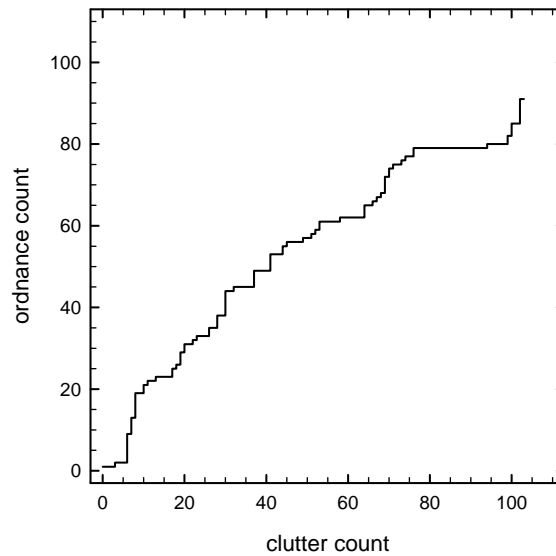


**Figure 20. ROC curve for the  $\chi^2$  weighting applied to the APG Blind Grid as shown in the left-hand side of Figures 25 and 26 of Reference 8.**

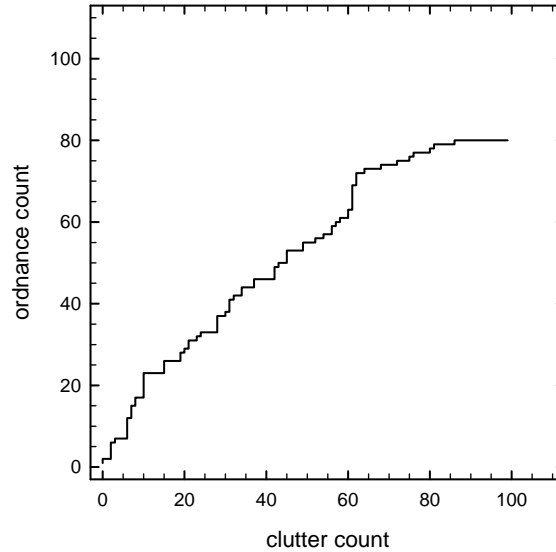


**Figure 21. ROC curve for the case of  $\chi^2$  weighting with an estimate of “bouncing noise” included applied to the APB Blind Grid.**

The  $\chi^2$  ratio method (Figure 22) does show some promise. Notice, however, that the curve in Figure 22 includes even fewer ordnance and clutter items than in Figure 21. The  $\chi^2$  ratio method requires two different inversions to converge to sensible results in order to calculate the ratio. As the SNR decreases, this becomes an increasingly difficult hurdle. Library methods such as this can work well when the expected targets are well defined but can provide inappropriate results when a munitions item not in the library is encountered.

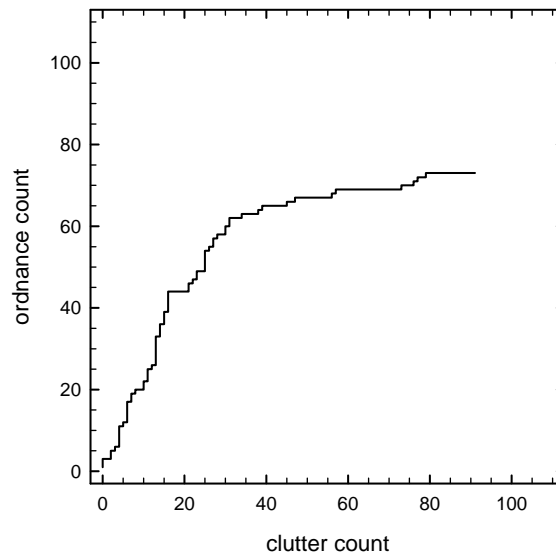


**Figure 22. ROC curve for the  $\chi^2$  ratio method applied to the APG Blind Grid.**

## 8.2 ABERDEEN PROVING GROUND OPEN FIELD

Selected results from our surveys at the Open Field at the APG Standardized Test Site have been provided to us by analysts at the IDA. These results are summarized graphically in the following sections.

### 8.2.1 Response Stage

Response stage data from the Open Field scenario at the APG Standardized Test Site is shown in Figure 23 as a plot of probability of detection versus normalized background alarm rate. There are two analysis models shown on the plot. The first, the red line, corresponds to considering only those targets that were covered by the survey and are not within 2 m of another target. The analysis corresponding to the blue line retains those limitations and also excludes those targets deeper than 11-times their diameter. We showed in Figure 17 that the GEM-3 array is able to detect down to depths of at least 11-times a target's diameter (and below for small to medium targets). Response stage results broken out by item type are shown in Figure 24. In this figure, the depth of 100% detection is denoted by the blue bar and the depth of maximum detection is shown as the horizontal line. For a number of the items, 105-mm HEAT for example, these two depths are the same. For the majority of the items, the maximum depth of detection is below the depth of 100% detection.

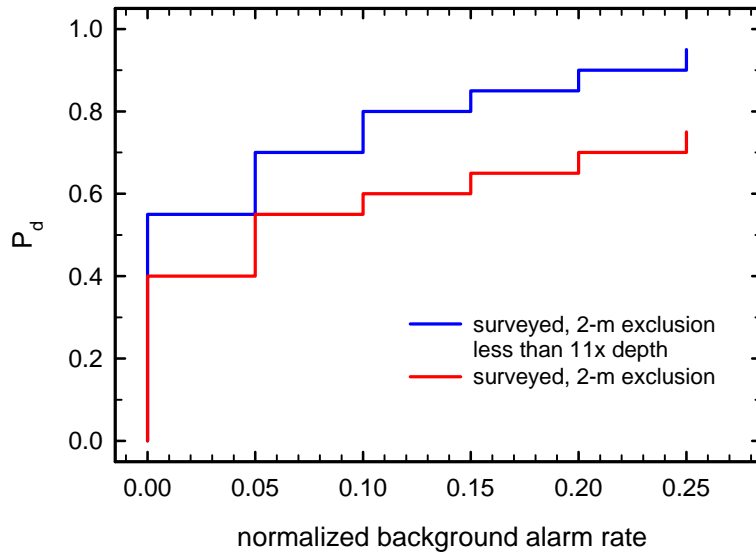


**Figure 23. Detection performance at the APG Open Field scenario.**

The red line is derived considering only targets that were covered in the survey and are not within 2 m of another target. The blue line retains those criteria and also excludes targets deeper than 11-times their diameter.

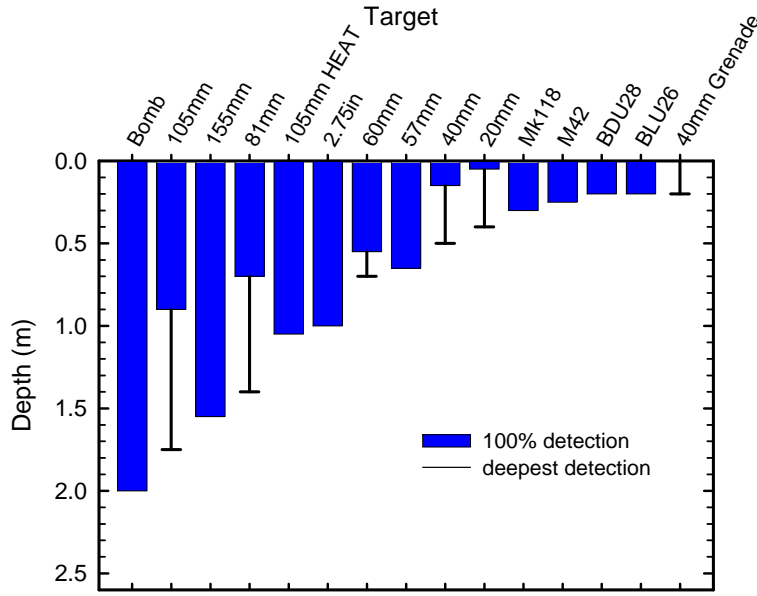


**Figure 24. Response stage results for the APG Open Field scenario broken out by target type.**

### 8.2.2 Discrimination Stage

Discrimination stage performance at the APG Open Field using the same two analysis models is shown in Figure 25. As above, the exclusion of items at depths below 11-times their diameter (presumably lower signal-to-noise [S/N] anomalies) improves the discrimination performance obtained.

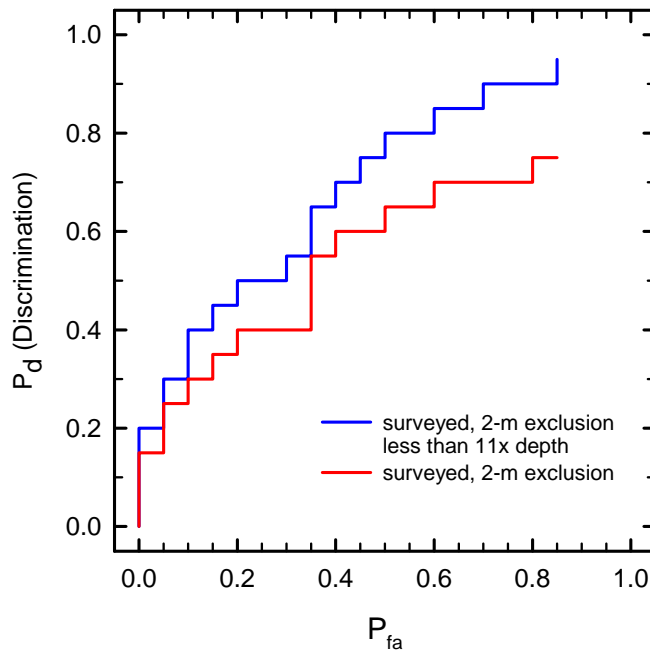


**Figure 25. Discrimination performance at the APG Open Field scenario.**

The red line is derived considering only targets that were covered in the survey and are not within 2 m of another target. The blue line retains those criteria and also excludes targets deeper than 11-times their diameter.

### 8.3 YUMA PROVING GROUND OPEN FIELD

Selected results from our surveys at the Open Field at the YPG Standardized Test Site have been provided to us by analysts at the IDA. These results are summarized graphically in the following sections.

#### 8.3.1 Response Stage

Response stage results for the YPG Open Field scenario are shown in Figures 26 and 27. As for APG, they are analyzed by excluding first items that were not covered by the survey or are within 2 m of another item, then retaining those exclusions and further excluding items deeper than 11-times their diameter. Notice that the background alarm rates in Figure 26 are more than a factor of two smaller than the corresponding results from Aberdeen. Although the Yuma site is more geologically active than Aberdeen, it is smoother so there were fewer false alarms due to platform bouncing over deep ruts. Detection depths at Yuma are, in general, in line with those obtained at Aberdeen. Note however, that a shallow bomb was apparently missed resulting in an unusual plot for that target type.

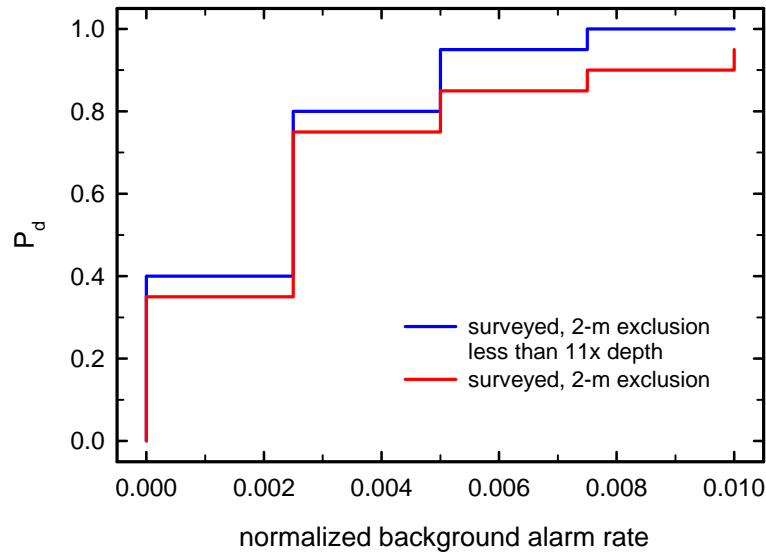


**Figure 26. Detection performance at the YPG Open Field scenario.**

The red line is derived considering only targets that were covered in the survey and are not within 2 m of another target. The blue line retains those criteria and also excludes targets deeper than 11-times their diameter.

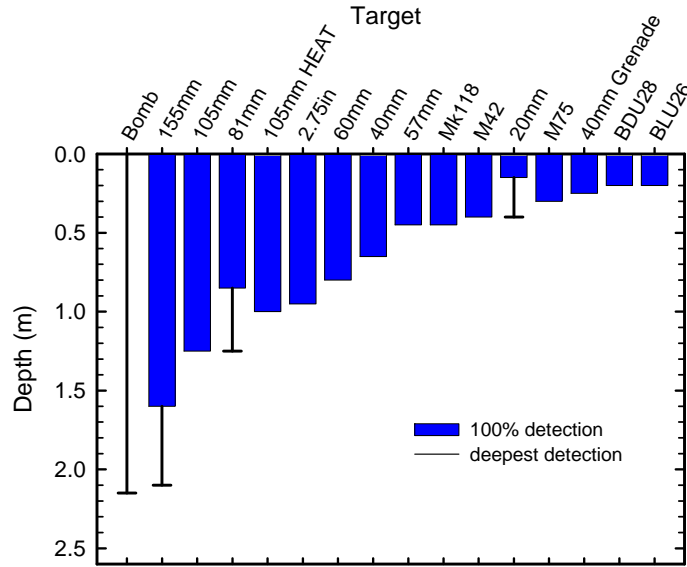


**Figure 27. Response stage results for the YPG Open Field scenario broken out by target type.**

### 8.3.2 Discrimination Stage

Discrimination Stage results from the YPG Open Field are shown in Figure 28. As before, exclusion of items that are deeper than 11-times their diameter improves performance, which is better on the whole than that observed at Aberdeen. As with the response stage, this is likely due to the lower platform motion noise observed at the Yuma site.

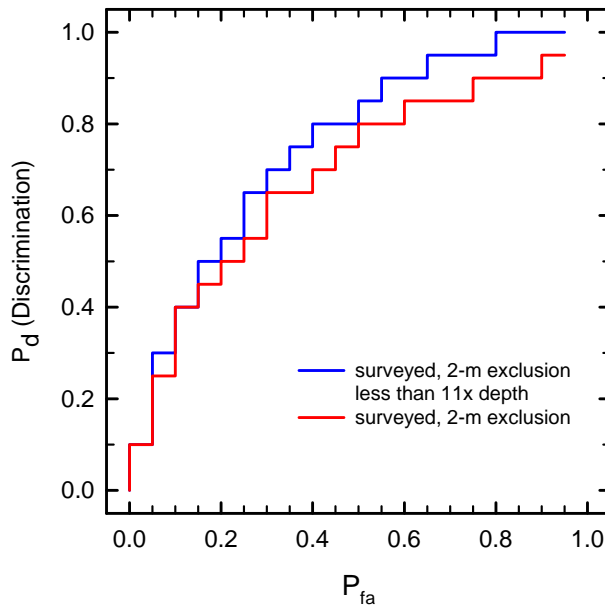


**Figure 28. Discrimination performance at the YPG Open Field scenario.**

The red line is derived considering only targets that were covered in the survey and are not within 2 m of another target. The blue line retains those criteria and also excludes targets deeper than 11-times their diameter.

## 9.0 COST ASSESSMENT

### 9.1 COST MODEL

The costs for a 50-acre survey using the GEMTADS array in discrimination mode are detailed in Table 10. These surveys require interleaved sampling, as was practiced in the two Standardized Test Site surveys. The coverage using this collection methodology is ~5 acres/7.5 hour survey day. Thus, a 50-acre survey requires two weeks in the field. All costs are estimated in FY 2006 dollars.

**Table 10. Summary of Costs for a 50-acre GEM array survey.**

Cost Category	Sub-Category	Cost	Sub-Total
Mobilization costs			\$63,500
	Preliminary site visit	\$8,000	
	Test plan preparation	\$10,000	
	Equipment prep and packing/unpacking	\$12,000	
	Rental trailer and transportation	\$17,500	
	Analysts setup	\$10,000	
	Real-time travel for 4 personnel	\$6,000	
Logistics (if required)			\$13,600
	Establish GPS control points	\$4,000	
	Office and garage trailers, portable toilets	\$2,350	
	Generator/fuel/electrician	\$4,000	
Operating costs (2-week survey)	Materials	\$3,250	
			\$59,500
	Supervisor	\$12,000	
	On-site analyst	\$9,500	
	Vehicle operator	\$6,100	
	Field technician	\$7,500	
	Per diem (4 personnel x 14 days x \$150)	\$8,400	
	Rental vehicles	\$4,000	
Equipment repair	\$12,000		
Analysis & reporting			\$25,000
Total cost			\$161,600

### 9.2 COST DRIVERS

Two factors were expected to be strong drivers of cost for this technology as demonstrated. The first is the acreage that can be surveyed per day. The actual acreage covered sets the amount of data collected per day. Higher productivity in data collection equates to more total acreage covered for a given period of time in the field. The time required for selecting and analyzing individual anomalies can be significantly higher than other, traditional methods and could become a cost driver due to the time involvement. The thoughtful use of available automation techniques for individual anomaly analysis with operator QC support can moderate this effect.

### 9.3 COST BENEFIT

The main benefit to using a UXO classification process is cost-related. The ability to reduce the number of nonhazardous items that have to be dug or dug as hazardous directly reduces the cost

of a remediation effort. The additional information for anomaly classification provided by the GEMTADS array provides additional information for the purposes of anomaly classification. If there is buy-in from the stakeholders to use these techniques, this information can be used to reduce costs.



## 10.0 IMPLEMENTATION ISSUES

Implementation of the methods used in this demonstration requires additional survey time compared to a minimum-effort detection survey. We have shown that the MTADS can detect all UXO of gauges 40 mm or larger with a total-field magnetometry survey alone. For ordnance target sets that include 60- and 81-mm mortars at depths of 0.75 to 1 m and/or 20- and 30-mm submunitions, an overlapping EMI survey is required to get a high detection probability. Compared to the magnetometer array, we use two interleaved GEM-3 array surveys to ensure sufficient data density over each target to get a reliable fit to our models. This increases the survey hours onsite although it does not impact the mobilization and data analysis costs. In many cases, the extra survey costs are equivalent only to the cost of digging one or two additional targets per acre.

Discrimination-quality data collection requires either interleaved sampling (in the case of the GEM-3 array) or more rigorously surveying in two orthogonal directions (in the case of the EM61 array). This requires another factor of two penalty on the EM systems for an overall productivity reduction of a factor of four. The sensor transmitters used for the GEM-3 sensor in the demonstrated array are fired in a sequential pattern unlike the MTADS EM61 array where the sensor transmitters are synchronized for maximum transmit moment. Because the EM61 array transmitters are synchronized, the interleaved survey passes must be orthogonal as well to ensure both sufficient data density and sufficient target illumination. The sequential transmitter pattern of the GEM-3 array removes the orthogonality constraint, which can be onerous on some sites, and terrain such as on a steep hill face.

The GEMTADS array is a vehicular-towed array with the operating limitations of a towed system. Support requirements are not extensive. For normal operation, the vehicle and sensor trailer are stored in a garage or similar space overnight; this has often been a two-door Conex trailer. AC power is required at the storage site to charge the vehicle batteries overnight. Other batteries (sensors, GPS base station, radios, etc.) can be charged off site or in a hotel room but, of course, it is most convenient to charge them at the storage site. For extended surveys, an office space for the data preprocessor and to serve as an electronics diagnosis and repair area is suggested. All of this support was provided at the Standardized Test Sites, requiring no additional action for the demonstration.

The minimum survey crew consists of a vehicle driver, one other field helper (for safety considerations), and a data QC and preprocessing analyst. The surveys described in this report included an additional member of the team who split time between the field, data preprocessing, and general troubleshooting. As the data preprocessor has time available, target analysis can begin in the field. The bulk of target analysis is carried out later at the analyst's office.

*This page left blank intentionally.*

## 11.0 REFERENCES

1. "Report of the Defense Science Board Task Force on Unexploded Ordnance," December 2003, Office of the Under Secretary of Defense for Acquisition, Technology, and Logistics, Washington, D.C. 20301-3140, <http://www.acq.osd.mil/dsb/uxo.pdf>.
2. "Survey of Munitions Response Technologies," ESTCP, ITRC, and SERDP, June, 2006.
3. "Jefferson Proving Ground Technology Demonstration Program Summary," G. Robitaille, J. Adams, C. O'Donnell, and P. Burr, <http://aec.army.mil/usaec/technology/jpgsummary.pdf>.
4. "Frequency-Domain Electromagnetic Induction Sensors for the Multi-Sensor Towed Array Detection System," H. H. Nelson, B. Barrow, T. Bell, R. S. Jones, and B. SanFilipo, NRL/MR/6110—02-8650, November 2002.
5. "Electromagnetic Induction and Magnetic Sensor Fusion for Enhanced UXO Target Classification," H. H. Nelson and Bruce Barrow, NRL/PU/6110--00-423.
6. "Quantification of Noise Sources in EMI Surveys, Technology Demonstration Report, Army Research Laboratory Blossom Point, Maryland, July – September, 2006," G.R. Harbaugh, D.A. Steinhurst, M. Howard, B.J. Barrow, J.T. Miller, and T.H. Bell, NRL Memorandum Report NRL/MR/6110—10-9235, Naval Research Laboratory, Washington, DC, January 14, 2010.
7. See website: <http://aec.army.mil/usaec/technology/uxo01c03.html> for more details. A complete list of Standardized Target Repository items is available at: <http://aec.army.mil/usaec/technology/uxo-stdtargets.pdf>.
8. "Enhanced UXO Discrimination Using Frequency-Domain Electromagnetic Induction," ESTCP MM-0033 Final Report, submitted May, 2007. H. Nelson, D. Steinhurst, B. Barrow, T. Bell, N. Khadr, W. San Filipo, I. Won.
9. "Moving Platform Orientation for an Unexploded Ordnance Discrimination System," D. Steinhurst, N. Khadr, B. Barrow, and H. Nelson, GPS World, 2005, 16/5, 28 – 34.
10. "Airborne MTADS Demonstration at the Badlands Bombing Range, September, 2001," J.R. McDonald, D.J. Wright, N. Khadr, H.H. Nelson, NRL/PU/6110—02-453.
11. "Standardized UXO Technology Demonstration Site Blind Grid Scoring Record No. 127," L. Overbay, ATC-8740, Aberdeen Test Center, MD, January, 2004.
12. "Standardized UXO Technology Demonstration Site Open Field Scoring Record No. 675," L. Overbay and G. Robitaille, ATC-8974, Aberdeen Test Center, MD, August, 2005.
13. "Standardized UXO Technology Demonstration Site Blind Grid Scoring Record No. 213," ATC-8836, Aberdeen Test Center, MD, January, 2005.

14. “Standardized UXO Technology Demonstration Site Open Field Scoring Record No. 245,” L. Overbay, ATC-8942, Aberdeen Test Center, MD, March, 2005.

## APPENDIX A

### POINTS OF CONTACT

Point of Contact	Organization	Phone Fax E-Mail	Role
Dr. Jeff Marqusee	ESTCP Program Office 901 North Stuart Street, Suite 303 Arlington, VA 22203	703-696-2120 (V) 703-696-2114 (F) jeffrey.marqusee@osd.mil	Director, ESTCP
Dr. Anne Andrews	ESTCP Program Office 901 North Stuart Street, Suite 303 Arlington, VA 22203	703-696-3826 (V) 703-696-2114 (F) anne.andrews@osd.mil	Deputy Director, ESTCP
Dr. Herb Nelson	ESTCP Program Office 901 North Stuart Street, Suite 303 Arlington, VA 22203	703-696-8726 (V) 703-696-2114 (F) 202-215-4844 (C) herbert.nelson@osd.mil	Program Manger, MM
Dr. Dan Steinhurst	Nova Research, Inc. 1900 Elkin Street, Suite 230 Alexandria, VA 22308	202-767-3556 (V) 202-404-8119 (F) 703-850-5217 (C) dan.steinhurst@nrl.navy.mil	PI and Quality Assurance Officer
Mr. Glenn Harbaugh	Nova Research, Inc. 1900 Elkin Street, Suite 230 Alexandria, VA 22308	804-761-5904 (V) roo749@yahoo.com	Site Safety Officer
Dr. Tom Bell	SAIC 1225 S. Clark Street, Suite 800 Arlington, VA 22202	702-414-3904 (V) thomas.h.bell@saic.com	Data Analyst
Dr. Nagi Khadr	SAIC 1225 S. Clark Street, Suite 800 Arlington, VA 22202	217-531-9026 (V) nagi.khadr@saic.com	Data Analyst
Dr. Bruce Barrow	SAIC 1225 S. Clark Street, Suite 800 Arlington, VA 22202	703-414-3884 (V) bruce.j.barrow@saic.com	Data Analyst
Dr. I.J. Won	Geophex, 605 Mercury Street Raleigh, NC 27603-2343	919-839-8515 (V) 919-839-8528 (F) ijwon@geophex.com	President, Geophex

*This page left blank intentionally.*



## ESTCP Program Office

901 North Stuart Street  
Suite 303  
Arlington, Virginia 22203  
(703) 696-2117 (Phone)  
(703) 696-2114 (Fax)  
E-mail: [estcp@estcp.org](mailto:estcp@estcp.org)  
[www.estcp.org](http://www.estcp.org)